Carbon and nitrogen cycling in Yedoma permafrost controlled by microbial functional limitations

Carbon and nitrogen cycling in Yedoma permafrost controlled by microbial functional limitations

Sylvain Monteux[1,2‡*], Frida Keuper[1,3‡*], Sébastien Fontaine[4], Konstantin Gavazov[1,5], Sara Hallin[6], Jaanis Juhanson[6], Eveline J. Krab[1,2], Sandrine Revaillot[4], Erik Verbruggen[7], Josefine Walz[1], James T. Weedon[7,8], Ellen Dorrepaal[1].

* Corresponding authors

‡ These authors contributed equally

Author affiliations

1: Climate Impacts Research Centre – Department of Ecology and Environmental Sciences – Umeå University. 98107 Abisko, Sweden.

2: Department of Soil and Environment – Swedish University of Agricultural Sciences (SLU). 75007 Uppsala, Sweden.

3: BioEcoAgro Joint Research Unit, INRAE, F-02000 Barenton-Bugny, France.

4: UMR Écosystème Prairial – INRAE, VetAgro Sup. F-63000 Clermont-Ferrand, France.

5: Swiss Federal Institute for Forest, Snow and Landscape Research (WSL). 1015 Lausanne, Switzerland.

6: Department of Forest Mycology and Plant Pathology – Swedish University of Agricultural Sciences (SLU). 75007 Uppsala, Sweden.

7: Plants and Ecosystems – Department of Biology – Universiteit Antwerpen. 2610 Wilrijk, Belgium.

8: Systems Ecology – Department of Ecological Sciences – Vrije Universiteit Amsterdam. 1081 HV Amsterdam, The Netherlands.

Summary

Warming-induced microbial decomposition of organic matter in permafrost soils constitutes a climate-change feedback of uncertain magnitude. While physico-chemical constraints on soil functioning are relatively well understood, the constraints attributable to microbial community composition remain unclear. Here we show that biogeochemical processes in permafrost can be impaired by missing functions in the microbial community – functional limitations – likely due to environmental filtering of the microbial community over millennia-long freezing. We inoculated Yedoma permafrost with a functionally diverse exogenous microbial community to test this mechanism by introducing potentially missing microbial functions. This initiated nitrification activity and increased CO_2 production by 38% over 161 days. The changes in soil functioning were strongly associated with an altered microbial community composition, rather than with changes in soil chemistry or microbial biomass. The present permafrost microbial community composition thus constrains carbon and nitrogen biogeochemical processes, but microbial colonization, likely to occur upon permafrost thaw *in situ*, can alleviate such functional limitations. Accounting for functional limitations and their alleviation could strongly increase our estimate of the vulnerability of permafrost soil organic matter to decomposition and the resulting global climate feedback.

Main

Permafrost soils store large amounts of organic matter (1100-1500 Pg-C[1]; 66 Pg-N[2]) and degradation of this organic matter can accelerate global warming. The vulnerability of the permafrost carbon pool to increased microbial mineralization with global warming has typically been estimated by incubating permafrost soil in isolation from the overlying topsoil[3–5]. Such studies generally focus on climatic, physical and soil chemical constraints on biogeochemical processes, and constraints by microbial community composition have been given less attention. The impairment or absence of a biogeochemical process due to absence or low abundance of the microbial taxa involved, is often ignored as a determinant of carbon and nitrogen cycling because soil microbial communities are usually considered functionally-redundant[6]. This presumed absence of functional limitations in microbial communities is typically deduced from the high diversity and dispersal capacity of soil microbes[7,8], the weak coupling between their taxonomy and phenotype[9], and because soil physical and chemical properties affect both biogeochemical process rates and microbial community composition simultaneously[10]. Empirical evidence shows that changes in microbial community composition rarely associate with changes in ecosystem processes carried out by many taxa, although such associations are more common for changes in less redundant functions[11–13]. However, in permafrost soils, freezing conditions and associated dispersal limitations[14,15] have imposed a strong environmental filter over millennial time scales, which has likely reduced the diversity of the *in situ* microbial communities[15,16], and potentially their functional repertoire[14]. Permafrost soil microbial communities might therefore be functionally limited, especially for functions performed by rare taxa which are more sensitive to diversity loss[12,17]. Upon deepening of the thaw-front[18,19] or permafrost collapse, dispersal and colonization by functionally-diverse communities from the overlying topsoil[20,21] or airborne microbes[7,22] are no longer hindered, which might relieve such functional limitations. Studies with permafrost soil layers incubated in isolation [e.g. 3,23,24] quantify the response of communities that retain their potential functional limitations. If permafrost microbial communities

have functional limitations, this response to thawing, and thus the estimate of the vulnerability of permafrost carbon and nitrogen, might be biased. We hypothesized that functional limitations occur in permafrost microbial communities, and consequently that the introduction of diverse exogenous microorganisms would alter their functioning.

We tested whether microbial communities in Upper Pleistocene Yedoma permafrost are functionally limited in carbon and nitrogen cycling processes, by comparing CO_2 production and changes in inorganic nitrogen pools between control and inoculated Yedoma permafrost. Organic-rich deposits in the Yedoma domain store around 25% of permafrost frozen C stocks, 213 ± 24 Pg-C[1,25], of which, based on incubations, ~10% is especially decomposable[25]. Inoculation consisted in replacing 2.5% permafrost (w:w) by a donor soil harbouring a previously characterized, functionally diverse microbial community[26,27], to maximise the potential effect on the permafrost microbial community composition and the possibility of functional rescue (hereafter referred to as 'Soil transfer', Extended Data Figure 1). In the absence of functional limitation, we expected little to no effect of this soil transfer on carbon and nitrogen related processes despite changes in microbial community composition, while changes in carbon and nitrogen related processes would reveal functional limitations.

Soil transfer modified microbial community trajectory

Soil transfer (ST) induced changes in bacterial and fungal communities, which persisted throughout the 161-day incubation (Figure 1, Extended Data Figure 2). This was reflected by differences in bacterial community composition (ManyGLM ANOVA, $P < 0.01$, Figure 1a and b, Extended Data Figure 3), and by a doubling of α-diversity (Figure 1c). More specifically, the relative abundance of 33% of the 4768 bacterial OTUs (79% of the reads) differed significantly between control and ST samples over the incubation period. The fungal community composition was less dramatically

modified, but α-diversity tripled (Extended Data Figure 2, Extended Data Figure 3). The large and persistent changes in community composition, resembling neither the donor nor the control samples after 161 days, show that permafrost microbial communities are vulnerable to coalescence (*sensu* Ref [28]: the joining of previously separate communities). Therefore, permafrost microbial communities do not only respond intrinsically to thawing, as previously observed[29], but are also sensitive to colonization by other microbial taxa (e.g. from the overlying active layer), with potentially major consequences for the trajectory of their response to thawing.

Functional limitation of CO_2 production

CO_2 production rates increased on average by 41% (95% CI: 30-52%, n=15, Figure 2a) in inoculated relative to control samples. Accounting for fluctuations over time (time : ST interaction n.s., Extended Data Figure 3), we observed a 38% increase in cumulative aerobic CO_2 production over the 161 day incubation (95% CI: 25-52%, n=3, two-sided Welch's $t_{2,12}$=11.76, P=0.006). This coincided with a net loss of total dissolved carbon (TDC) in the ST samples (Figure 2b, Extended Data Figure 3), but the difference in TDC between ST and control treatments was 33% smaller than the difference in CO_2 production (95% CI: 16-49%, n=15, ANOVA $F_{1,20}$=17.11, P<0.001; Extended Data Figure 4). The small quantity of transferred soil (2.5%) did not introduce enough C, nutrients or microbial biomass to initially affect the soil chemistry, microbial biomass, or explain the increase in CO_2 production (Figure 2, Extended Data Figures 1, 3, 5, Supplementary Discussion) and the basal CO_2 production of the donor soil was 65% lower than that of the control samples (Extended Data Figure 6). Further, permafrost organic matter-derived CO_2 production was not affected by nutrient (NPK) amendment and only moderately by labile carbon amendment (^{13}C-cellulose, *c*. 9% increase) and these effects were additive to effects of soil transfer (no interaction effects, Supplementary Discussion, Extended Data Figure 6).

The increased CO_2 production rates were predominantly associated with relative abundances of different bacterial taxa and abundance of microbes involved in ammonia oxidation rather than with soil chemistry or microbial biomass (Table 1; RandomForest-based variable selection, Extended Data Figure 7). Among the 27 most important variables, 23 reflected information on the microbial communities. These results strongly suggest that the exogenous change in microbial community composition caused the increase in CO_2 emissions. Functional limitations and functional alleviations related to the composition of the microbial community can therefore influence broad ecosystem processes, such as CO_2 production, in Yedoma permafrost.

Functional limitation of nitrification

Soil transfer (ST) drastically altered the composition of nitrogen species in the dissolved inorganic nitrogen (DIN) pool (Figure 2c-d), although the total DIN content only marginally increased (Extended Data Figure 3). Ammonium content in the permafrost was initially high (Figure 2c), similar to what has been observed previously for other permafrost types[30,31], whereas nitrate and nitrite content was initially below the detection limit (*c*. 0.5 mg-N . kg-dry-soil^{-1}). In the ST samples only, nitrate and nitrite were detectable after 15 days and then strongly increased (Figure 2d, Extended Data Figure 3), while the ammonium content concomitantly almost halved over the 161 day incubation (Figure 2c, Extended Data Figure 3).

The abundance of *amoA* genes, coding for the ammonium monooxygenase in Thaumarchaeota and Betaproteobacteria, were below detection limit in control samples, but were introduced upon soil transfer (Figure 3). By day 161, bacterial *amoA* had reached the same amounts as observed in the donor soil (Figure 3b, Supplementary Discussion). Accordingly, *Nitrosomonadaceae* OTUs had a higher abundance in ST samples (Figure 1a) and their relative abundance was strongly correlated with the nitrate and nitrite pools (Pearson's r = 0.78; 95% CI 0.57–0.89; $P < 10^{-5}$; n = 29). Clade A and B

amoA from complete ammonia oxidisers (comammox) within the bacterial phylum *Nitrospira*[32] were detected in all ST and control samples from 15 days onwards, but reliable quantitative data on comammox were not obtained (Supplementary Table 1). Nevertheless, the qualitative data indicate minor differences between control and ST samples and no changes after day 15. In support, relative abundances of detected *Nitrospirae* OTUs were not correlated with the onset of nitrification (r = -0.03; 95% CI -0.39–0.34; $P = 0.885$; n = 29). The introduction of large numbers of bacterial-*amoA* genes, and, to a lesser extent, archaeal-*amoA* genes, together with the onset of nitrification upon soil transfer, thus confirms that community coalescence-induced introduction of bacterial ammonia oxidizers alleviated the functional limitation of nitrification.

Proposed mechanisms and implications

Our results demonstrate that microbial community composition can limit microbially driven mineralization processes in thawing permafrost soils, affecting both carbon and nitrogen cycling processes with potential climate feedbacks. Long-term residence under unfavourable conditions in the permafrost likely resulted in impaired or complete loss of functions over time. The nitrifier abundance, reflected by the *amo*A genes, was sufficiently low to impede nitrification, potentially because of the prevailing anoxic conditions and because this function is carried out by a few, rare and phylogenetically constrained taxa. However, even processes performed by presumably redundant, broad groups of microorganisms, such as those involved in CO_2 production, appear constrained by the composition of the microbial community. Together, these results suggest that genetic capacity needed for coping with thawed conditions was lost, or absent upon permafrost aggradation, from the community. This functionally limited community was, however, vulnerable to coalescence, as contact with an exogenous community modified the trajectory of its compositional change over time. When coalescence with a functionally diverse community occurs, like in the present study, exogenous taxa

with their genetic capacity seem to be able to alleviate functional limitations and thereby diversify soil functioning.

The consequences for soil functioning during *in situ* thaw will depend on the manner in which new microbial communities will colonize newly thawed permafrost soil, and on the extent to which these communities can alleviate functional limitations. Colonization can occur through deepening of the active layer, i.e. the seasonally thawed soil above the permafrost, *via* extended root-growth or percolating water[18,19] and may additionally occur through airborne dispersal[7,22] or soil mixing upon permafrost collapse (cryoturbation[33], thermokarst[34], thermo-erosion[25], and active layer detachment[35]). Our observations suggest that colonization could happen rapidly upon thawing. Since tundra active layer soil communities can be as functionally-diverse as those found in temperate grasslands[20] (such as our donor soil), and because microorganisms carrying out nitrification, for instance, have been detected close to the permafrost table[21,36], it seems likely that active layer communities can alleviate functional limitations. To test this assumption, we reproduced our main experiment, by inoculating Yedoma permafrost with suspensions of arctic topsoils that can be found in the Yedoma domain[25] (Extended Data Figure 8a). The arctic topsoil inoculations substantially increased CO_2 production, although to a lesser extent than the donor soil used in our main experiment. We further explored generalization beyond our Upper Pleistocene study system by inoculating three more recent (Holocene) permafrost soils with our donor soil, and in agreement with our main experiment, CO_2 production increased in all inoculated samples (+20-37%, Extended Data Figure 8b). Overall, our findings strongly suggest that, upon thaw, microbial colonizers could rapidly change the metabolic potential of permafrost microbial communities.

The increase in CO_2 release and the initiation of nitrification after relieving functional limitations highlights microbial community dynamics as an important but poorly understood source of non-

linearity in the relation between warming, permafrost thaw and changes to Earth's radiative forcing. Our results imply that incubation-based predictions of future soil organic matter turnover in permafrost affected soils likely underestimate the magnitude of the permafrost carbon-climate feedback. Not only can CO_2 production and nitrification activity increase, but the introduction of nitrifiers from the active layer will pave the way for denitrification or nitrifier denitrification, further increasing radiative forcing through the production of the potent greenhouse gas nitrous oxide[31,37–40]. The presence or absence of nitrogen processing functions may also affect primary production by altering plant-microbe competition for the presumably large pool of newly thawed permafrost nitrogen[30,41,42] or increasing its leaching into aquatic ecosystems[43]. Although we only tested for a limited set of functions, more soil processes may be subject to functional limitation, which could explain recent findings on the varying methanogenesis potential in permafrost soils[44,45]. Demonstrating the existence and alleviation of functional limitations in permafrost microbial communities is a first step towards apprehending its extent and consequences in natural settings. Understanding how small-scale soil processes, such as changes in microbial community composition and soil chemistry, affect functional limitations in permafrost, their alleviation upon thawing, and its consequences for carbon and nitrogen biogeochemistry, is urgent to improve global climate feedback predictions.

References

1. Hugelius, G. *et al.* Estimated stocks of circumpolar permafrost carbon with quantified uncertainty ranges and identified data gaps. *Biogeosciences* **11**, 6573–6593 (2014).

2. Harden, J. W. *et al.* Field information links permafrost carbon to physical vulnerabilities of thawing. *Geophys. Res. Lett.* **39**, L15704 (2012).

3. Schädel, C. *et al.* Circumpolar assessment of permafrost C quality and its vulnerability over time using long-term incubation data. *Glob. Change Biol.* **20**, 641–652 (2014).

4. Schuur, E. A. G. *et al.* Climate change and the permafrost carbon feedback. *Nature* **520**, 171–179 (2015).

5. Koven, C. D. *et al.* A simplified, data-constrained approach to estimate the permafrost carbon–climate feedback. *Philos. Trans. R. Soc. Math. Phys. Eng. Sci.* **373**, 20140423 (2015).

6. Nannipieri, P. *et al.* Microbial diversity and soil functions. *Eur. J. Soil Sci.* **68**, 12–26 (2003).

7. Harding, T., Jungblut, A. D., Lovejoy, C. & Vincent, W. F. Microbes in High Arctic Snow and Implications for the Cold Biosphere. *Appl. Environ. Microbiol.* **77**, 3234–3243 (2011).

8. Thompson, L. R. *et al.* A communal catalogue reveals Earth's multiscale microbial diversity. *Nature* **551**, 457–463 (2017).

9. Bier, R. L. *et al.* Linking microbial community structure and microbial processes: an empirical and conceptual overview. *FEMS Microbiol. Ecol.* **91**, fiv113 (2015).

10. Nunan, N., Leloup, J., Ruamps, L. S., Pouteau, V. & Chenu, C. Effects of habitat constraints on soil microbial community function. *Sci. Rep.* **7**, 4280 (2017).

11. Graham, E. B. *et al.* Microbes as Engines of Ecosystem Function: When Does Community Structure Enhance Predictions of Ecosystem Processes? *Front. Microbiol.* **7**, 214 (2016).

12. Schimel, J. Ecosystem Consequences of Microbial Diversity and Community Structure. in *Arctic and Alpine Biodiversity: Patterns, Causes and Ecosystem Consequences* 239–254 (Springer, Berlin, Heidelberg, 1995). doi:10.1007/978-3-642-78966-3_17.

13. Schimel, J. & Schaeffer, S. M. Microbial control over carbon cycling in soil. *Terr. Microbiol.* **3**, 348 (2012).

14. Bottos, E. M. *et al.* Dispersal limitation and thermodynamic constraints govern spatial structure of permafrost microbial communities. *FEMS Microbiol. Ecol.* **94**, fiy110 (2018).

15. Jansson, J. K. & Tas, N. The microbial ecology of permafrost. *Nat. Rev. Microbiol.* **12**, 414–425 (2014).

16. Mackelprang, R. *et al.* Microbial survival strategies in ancient permafrost: insights from metagenomics. *ISME J.* **11**, 2305–2318 (2017).

17. Philippot, L. *et al.* Loss in microbial diversity affects nitrogen cycling in soil. *ISME J.* **7**, 1609–1619 (2013).

18. Monteux, S. *et al.* Long-term in situ permafrost thaw effects on bacterial communities and potential aerobic respiration. *ISME J.* **12**, 2129–2141 (2018).

19. Johnston, E. R. *et al.* Responses of tundra soil microbial communities to half a decade of experimental warming at two critical depths. *Proc. Natl. Acad. Sci.* **116**, 15096–15105 (2019).

20. Fierer, N. *et al.* Cross-biome metagenomic analyses of soil microbial communities and their functional attributes. *Proc. Natl. Acad. Sci.* **109**, 21390–21395 (2012).

21. Sanders, T., Fiencke, C., Hüpeden, J., Pfeiffer, E. M. & Spieck, E. Cold Adapted Nitrosospira sp.: A Potential Crucial Contributor of Ammonia Oxidation in Cryosols of Permafrost-Affected Landscapes in Northeast Siberia. *Microorganisms* **7**, 699 (2019).

22. Hill, K. A. *et al.* Processing of atmospheric nitrogen by clouds above a forest environment. *J. Geophys. Res. Atmospheres* **112**, D11301 (2007).

23. Knoblauch, C., Beer, C., Sosnin, A., Wagner, D. & Pfeiffer, E.-M. Predicting long-term carbon mineralization and trace gas production from thawing permafrost of Northeast Siberia. *Glob. Change Biol.* **19**, 1160–1172 (2013).

24. Wild, B. *et al.* Plant-derived compounds stimulate the decomposition of organic matter in arctic permafrost soils. *Sci. Rep.* **6**, 25607 (2016).

25. Strauss, J. *et al.* Deep Yedoma permafrost: A synthesis of depositional characteristics and carbon vulnerability. *Earth-Sci. Rev.* **172**, 75–86 (2017).

26. Wertz, S. *et al.* Maintenance of soil functioning following erosion of microbial diversity. *Environ. Microbiol.* **8**, 2162–2169 (2006).

27. Fontaine, S. *et al.* Stability of organic carbon in deep soil layers controlled by fresh carbon supply. *Nature* **450**, 277–280 (2007).

28. Rillig, M. C. *et al.* Interchange of entire communities: microbial community coalescence. *Trends Ecol. Evol.* **30**, 470–476 (2015).

29. Mackelprang, R. *et al.* Metagenomic analysis of a permafrost microbial community reveals a rapid response to thaw. *Nature* **480**, 368–371 (2011).

30. Keuper, F. *et al.* A frozen feast: thawing permafrost increases plant-available nitrogen in subarctic peatlands. *Glob. Change Biol.* **18**, 1998–2007 (2012).

31. Elberling, B., Christiansen, H. H. & Hansen, B. U. High nitrous oxide production from thawing permafrost. *Nat. Geosci.* **3**, 332–335 (2010).

32. Daims, H. *et al.* Complete nitrification by Nitrospira bacteria. *Nature* **528**, 504–509 (2015).

33. Gittel, A. *et al.* Distinct microbial communities associated with buried soils in the Siberian tundra. *ISME J.* **8**, 841–853 (2014).

34. Weiss, N. *et al.* Thermokarst dynamics and soil organic matter characteristics controlling initial carbon release from permafrost soils in the Siberian Yedoma region. *Sediment. Geol.* **340**, 38–48 (2016).

35. Inglese, C. N. *et al.* Examination of Soil Microbial Communities After Permafrost Thaw Subsequent to an Active Layer Detachment in the High Arctic. *Arct. Antarct. Alp. Res.* **49**, 455–472 (2017).

36. Wild, B. *et al.* Microbial nitrogen dynamics in organic and mineral soil horizons along a latitudinal transect in western Siberia. *Glob. Biogeochem. Cycles* **29**, 567–582 (2015).

37. Voigt, C. *et al.* Increased nitrous oxide emissions from Arctic peatlands after permafrost thaw. *Proc. Natl. Acad. Sci.* **114**, 6238–6243 (2017).

285 38. Wrage-Mönnig, N. *et al.* The role of nitrifier denitrification in the production of nitrous
286 oxide revisited. *Soil Biol. Biochem.* **123**, A3–A16 (2018).
287 39. Siljanen, H. M. P. *et al.* Archaeal nitrification is a key driver of high nitrous oxide emissions
288 from arctic peatlands. *Soil Biol. Biochem.* **137**, 107539 (2019).
289 40. Voigt, C. *et al.* Nitrous oxide emissions from permafrost-affected soils. *Nat. Rev. Earth*
290 *Environ.* **1**, 420–434 (2020).
291 41. Keuper, F. *et al.* Experimentally increased nutrient availability at the permafrost thaw front
292 selectively enhances biomass production of deep-rooting subarctic peatland species. *Glob. Change*
293 *Biol.* **23**, 4257–4266 (2017).
294 42. Liu, X.-Y. *et al.* Nitrate is an important nitrogen source for Arctic tundra plants. *Proc. Natl.*
295 *Acad. Sci.* **115**, 3398–3403 (2018).
296 43. Myrstener, M. *et al.* Persistent nitrogen limitation of stream biofilm communities along
297 climate gradients in the Arctic. *Glob. Change Biol.* **24**, 3680–3691 (2018).
298 44. Knoblauch, C., Beer, C., Liebner, S., Grigoriev, M. N. & Pfeiffer, E.-M. Methane production
299 as key to the greenhouse gas budget of thawing permafrost. *Nat. Clim. Change* **8**, 309–312 (2018).
300 45. Holm, S. *et al.* Methanogenic response to long-term permafrost thaw is determined by
301 paleoenvironment. *FEMS Microbiol. Ecol.* **96**, fiaa021 (2020).
302
303
304 Correspondence and requests for materials should be addressed to Dr. Sylvain Monteux and Dr. Frida
305 Keuper.
306 Sylvain Monteux: Department of Soil and Environment, Swedish University of Agricultural Sciences
307 – PO Box 7014, SE-750 07 Uppsala, Sweden – Monteux@protonmail.com
308 Frida Keuper: BioEcoAgro Joint Research Unit, INRAE, Pôle du Griffon, 180 rue Pierre-Gilles de
309 Gennes, 02000 Barenton-Bugny, France – Frida.Keuper@inrae.fr

Acknowledgements

This study was funded by grants from the Wallenberg Academy Fellowship (KAW 2012.0152), Swedish Research Council (Dnr 621-2011-5444), Formas (Dnr 214-2011-788) and Kempestiftelserna (JCK-1822) all awarded to ED, by a grant from Formas (Dnr 2017-01182) awarded to EJK, by the European Union ClimMani COST Action (ES1308 COST ClimMani) Short Term Scientific Mission, the Arctic Research Centre at Umeå University (Arcum) strategic funding grants awarded to SM and by the Department of Forest Mycology and Plant Pathology, SLU. We thank Pr. Dr. Sarah Lebeer and the ENdEMIC team for hosting part of the molecular work, T. H. Douglas from the U.S. Army Cold Regions Research and Engineering Laboratory's Permafrost Tunnel (Alaska) for assistance and permission to sample, and the staff of Abisko Scientific Research Station for hospitality and logistic support.

Author contributions

SM, FK, SF, JTW and ED designed the study.

FK, SF, SM and SR performed the experiment.

SM, EV and JTW collected and analysed the DNA data.

FK and KG collected and analysed the PLFA data.

FK, SF, SM and SR collected and analysed all other data.

SM, JJ and SH collected and analyzed the qPCR data.

SM, FK, ED, SF, JW and EK designed and performed the experiment reproducing these findings as presented in Extended Data Fig 8.

SM and FK wrote the manuscript with contributions from all authors.

SM and FK contributed equally.

335 **Financial and non-financial competing interests statement**

336 The authors declare no competing interests.

337

338 **Figure captions**

339 **Figure 1: Changes in permafrost bacterial communities with inoculation by soil transfer (ST).**

340 **a**: Differential abundance of OTUs between ST and control samples over days 1-161 (n=15). Each

341 bar is a significantly changing OTU, a positive fold-change indicates a higher relative abundance in

342 ST. Crosses indicate the most abundant OTUs (>0.5% rarefied observations) and arrows indicate

343 nitrifiers. **b**: Phylum-/class-level summary of average relative abundances for control and ST samples.

344 **c**: Alpha-diversity (Abundance-based Coverage Estimator) of bacterial communities in control and

345 ST samples (mean ± SE). In **b** and **c**: n=3 except ST, day 1 where n=2; vertical lines separate pre-

346 incubation permafrost (control) and donor (left) soils from incubated soils (right).

347

348 **Figure 2: Changes in permafrost carbon and nitrogen fluxes and pools with soil transfer (ST).**

349 **a**: Daily CO_2 production rates at five dates (circles) and averaged over 161 days (bars). Numbers

350 indicate cumulative CO_2 production after 161 days. **b**: Total dissolved carbon content. **c**: Ammonium

351 content. **d**: Nitrate and nitrite content. (**a-d)**: light colour indicates control, dark colour ST (means ±

352 SE, n=3). Asterisks denote significant ST effect for averaged rates (**a**) or within a day (significant 'ST

353 x time' interaction; **b-c**). Letters indicate significant differences between days (main effect): ** $P \leq$

354 0.01; *** $P \leq 0.001$. Values in (**d**) for control (days 1-161) and ST (day 1) are below detection limit.

355

356 **Figure 3: Abundances of (a) archaeal and (b) bacterial *amoA* genes in permafrost inoculated by**

357 **soil transfer (ST) over 161 days.** Abundances of *amoA* genes for control samples (all days, **a-b**), as

358 well as two ST samples for bacteria (day 1, **b**) were below detection limit. Small symbols indicate

359 values for individual samples (average of two technical replicates), large symbols indicate means

(n=3), error-bars indicate standard-error of the mean (n=3) and different lower-case letters indicate significant differences between days (excluding pre-incubation). The black vertical lines separate pre-incubation donor soil (left, triangles) from incubated samples (right, circles).

Table 1: Explanatory power of multiple linear regressions of CO_2 production rates of Yedoma permafrost subjected or not to soil transfer.

Predictors	AICc	Adjusted R^2
Community-function	61.213	0.662
Community-function + Biomass	67.865	0.640
Community-function + Chemistry	72.875	0.655
Community-function + Biomass + Chemistry	82.823	0.634
Biomass + Chemistry	73.362	0.565
Biomass	72.088	0.438
Chemistry	76.170	0.433

CO_2 production rates are divided by the average of their respective date to omit the time dynamics and focus on the differences induced by soil transfer. Community-function: variables selected by the VSURF algorithm (bacterial and archaeal *amoA* genes abundance, Bacteroidetes and WS3 phyla relative abundance; Extended Data Figure 7); Biomass: proxies of microbial biomass (16S rRNA gene abundance, microbial biomass-C); Chemistry: soil chemistry variables (TDC, DIN, ammonium, nitrate+nitrite); AICc and R^2 are adjusted for differing number of parameters.

373 **Methods**

374 ***Soil description & sampling***

375 Deep (*c*. 20 m) Yedoma permafrost was collected in the CRREL Permafrost Tunnel Research Facility,
376 in Interior Alaska 11 km north of Fairbanks (64°57' N, 147°37' W). Yedoma deposits are ice- and
377 organic matter-rich, syngenetic permafrost, consisting of loess-like silt deposited during the
378 Pleistocene[46] and storing 181-407 Pg-C across the circum-Arctic[1,25]. They are sediments rather than
379 soil, but we use the term "soil" throughout the text for readability. The permafrost exposed in the
380 tunnel has been carbon dated at between 11 000 and 30 000 years BP[47,48]. For a more detailed
381 description of the Yedoma-permafrost and its microbial communities, see Refs. [16,49]. Three 40-cm
382 long, undisturbed silt cores from the lower silt unit were extracted from the tunnel wall with a SIPRE
383 corer, after excluding the first 20 cm to avoid cryodesiccated permafrost. The cores were kept frozen
384 during transport and stored until further processing at -15 °C.

385

386 We tested for the presence of the hypothesized functional limitations in Yedoma permafrost by
387 inoculating the permafrost samples with a donor soil harbouring a diverse microbial community,
388 following the logic that functions which only appeared or significantly increased upon soil transfer
389 were either absent or constrained in the original permafrost samples. Changing the microbial
390 community composition was central to our study design, thus we used solid soil transfer (2.5% w:w,
391 i.e. 0.5 g DW in 20 g) rather than inoculation by liquid suspension[50]. To cover a wide range of soil
392 functions we selected as donor a microbially diverse[20] temperate grassland soil with known
393 nitrification, denitrification[51], rhizosphere priming[27] capacity and high functional redundancy[26].
394 Elemental carbon and nitrogen content, and pH of this donor soil were similar to those of the Yedoma
395 samples (Extended Data Figure 1). The donor soil was collected from a temperate grassland (0-20 cm
396 depth) at the LTER research site of the French National Research Institute for Agriculture, Food and
397 the Environment (INRAE) in central France (Theix, 45°43' N, 03°01' E), from an abandonment-

398 treatment where no cutting or fertilizing had been carried out for 11 years. The soil is a drained
399 Cambisol developed on granitic rock and has been described in detail previously[26,27,51,52].
400
401 ***Soil transfer and incubation conditions, CO_2 production measurements and harvests***
402 Before starting the incubations, the permafrost was thawed at 5 °C, homogenized and mixed by
403 sieving, and pre-incubated for eleven days in a climate chamber (11 °C). We used clean, rather than
404 aseptic, conditions to keep our study similar, and therefore comparable, to other biogeochemistry-
405 oriented incubation studies [e.g. 23,24,53,54]. We assumed that potential contaminations would affect the
406 control and ST samples equally, and would in the worst case introduce functions missing from control
407 samples, thereby rendering our observations conservative. For each of 30 samples, approximately 32
408 g of pre-incubated Yedoma permafrost (fresh weight, equivalent to 20 g dry weight) was transferred
409 to 250 mL flasks sealed with rubber septa. Half of the flasks (15) were inoculated by soil transfer to
410 manipulate their microbial communities. The soil transfer (ST) consisted of replacing 2.5% (weight :
411 weight) of Yedoma samples with the donor soil described above (0.5 g DW-equivalent of donor soil
412 per 19.5 g DW-equivalent of Yedoma soil, Extended Data Figure 1), which incidentally replaced 2.5%
413 of initial soil C and N (15.25 mg-C and 1.2 mg-N) with 2.56% of initial C and 3.33% of initial N
414 (15.65 mg-C and 1.6 mg-N). Control jars average C and N content (610 mg-C and 48 mg-N) was
415 therefore similar to those in ST jars (610.4 mg-C and 48.4 mg-N), and both ST and control samples
416 were stirred to apply the same disturbance. We dark-incubated all flasks for up to 161 days at an
417 adjusted water potential of -100 kPa, under aerobic conditions and at 11 °C. This incubation
418 temperature is similar to summer active-layer temperatures in permafrost affected areas[30,55,56] and low
419 enough to be within the thermal tolerance range of psychrophilic microorganisms[57]. Headspace air
420 was sampled with a syringe at least once a week for the first 45 days, then at least once a month, to
421 measure CO_2 concentrations (Binos IRGA, Leybold-Hereaus, Germany). CO_2 production rates were
422 measured on one set of three flasks for each treatment for all time points until 161 days, except three

due to practical constraints. All flasks were flushed with moisturised CO_2-free air after each CO_2 production measurement, to ensure CO_2 concentrations in the flasks never reached 20,000 ppm. CO_2 concentrations were adjusted for changes in temperature and atmospheric pressure to calculate CO_2 production rates (τ) as follows:

$$\tau_{(i)} = \frac{[CO_2]_i \times (P_i V / RT_i)}{(\Delta_t)_i}$$

where $(\Delta_t)_i$ is the time interval between measurement ($_i$) and previous flushing, P_i is atmospheric pressure at measurement time, V the headspace volume, R the ideal gas constant and T_i the temperature. To calculate cumulative CO_2 production over the entire 161 days period, we multiplied each CO_2 production rate with the number of days since the previous flushing, within each jar. For time points when the 161-days set of flasks was not measured, we used linear interpolations of the CO_2 production rates between the previous and next measurements to estimate CO_2 production rates for intermediate incubation periods (Extended Data Figure 9), and used these in the calculations of cumulative CO_2 production. For reference, similar CO_2 production measurements were also performed on the donor soil used for soil transfer (in this case, supplemented with nutrients i.e. NH_4NO_3-KH_2PO_4, as in Ref. [52]), and on control and ST permafrost samples amended with nutrients and/or ^{13}C-labeled cellulose (Extended Data Figure 6, Supplementary Discussion and Supplementary Methods).

After each of 1, 15, 30, 71 and 161 days, three flasks of each treatment (control and ST) were destructively sampled for chemical and microbial analyses described below. Chemical analyses were carried out immediately, while two subsamples of ca. 3 g of soil were collected and kept frozen (-80 ºC) or lyophilized until DNA or PLFA extractions, respectively, were carried out.

448 ***Soil chemistry***

449 Soil samples from each treatment (n = 3) on days 1, 15, 30, 71 and 161 were analysed for total
450 dissolved carbon (TDC, dissolved organic carbon + dissolved inorganic carbon), dissolved inorganic
451 nitrogen (DIN: NH_4^+ and sum of NO_3^-/NO_2^-) and microbial biomass carbon. DIN, NH_4^+ and sum of
452 NO_3^-/NO_2^- were quantified in filtered extracts (5 g fresh weight in 30 mL 1 M KCl, 1 hour shaking)
453 and analysed on a San++ autoanalyzer (Skalar Analytical, Breda, The Netherlands). Similar extracts
454 (30 mM K_2SO_4) were used to quantify TDC, as well as microbial biomass carbon by the chloroform
455 fumigation-extraction method[58] followed by element-analyses of the lyophilised extracts. Microbial
456 biomass carbon (C_{MB}) was calculated using: $C_{MB} = E/k$, where k is the coefficient of extraction
457 efficiency (0.45; Ref. [58,59]) and E is the soluble microbial carbon, calculated as the difference between
458 organic carbon extracted by K_2SO_4 from fumigated and non-fumigated samples.

459

460 ***DNA extraction and quantitative PCR***

461 DNA was extracted using MoBio PowerSoil DNA extraction kits (now DNEasy PowerSoil Kit,
462 Qiagen, Venlo, The Netherlands), according to the manufacturer's instructions using 0.25 to 0.40 g of
463 soil, sampled 1, 15, 30, 71 and 161 days after the start of the incubation. Presence, quality and
464 concentration of DNA were assessed using a NanoDrop ND-1000 spectrophotometer (Thermo
465 Scientific, Waltham, Massachusetts), prior to amplicon preparation and further quantified using Qubit
466 2.0 (Invitrogen, Thermo Scientific) before performing quantitative real-time PCR (qPCR). With
467 Qubit, DNA concentrations ranged from 0.2 to 183 ng μL^{-1}.

468

469 To determine the genetic potential for nitrification, qPCR of variants of the functional gene *amoA*
470 found in betaproteobacterial ammonia oxidising bacteria (AOB[60]), ammonia oxidising archaea
471 (AOA[61]) within Thaumarchaeaota, complete ammonia oxidisers (comammox) within the phylum
472 Nitrospira (universal[62] and clade-specific[63]) were performed, as well as the abundance of the V3

region of the bacterial 16S rRNA gene as a proxy for bacterial abundance[64]. DNA extracts were diluted to 1 ng μL^{-1} (or 1:8 for samples below 4 ng μL^{-1}). Two 15 µL reactions per gene were analysed on independent runs using CFX Connect or CFX-96 Real-Time System thermocyclers (Bio-Rad laboratories, Hercules, California), and the conditions described in Supplementary Table 1. Each reaction contained 2 µL of diluted DNA template, 10 µg bovine serum albumin, 1x Biorad iQ™ SYBR®Green Supermix (Bio-Rad laboratories) and primers according Supplementary Table 1. The absence of polymerase inhibitors was ensured by amplifying a known amount of pCR 4-TOPO plasmid (Invitrogen) added to the DNA extracts or no-template controls and comparing the threshold cycle number. No inhibition of the amplification reactions was detected with the amount of DNA used.

Bacterial 16S rRNA and fungal ITS amplicon sequence libraries

We amplified the V3 region of the 16S ribosomal RNA to characterize bacterial communities for all samples (341F, 518R; Ref. [65]), and the internal transcribed spacer ITS1 region for fungal communities (ITS1f, ITS2; Ref. [66]) in samples from day 1, 15 and 161. DNA extracts were diluted to 5 ng μL^{-1} or 1:1, and up to 1:50 if amplification failed (samples that did not show visible amplification despite dilution were nevertheless used in the downstream processing). Primers and conditions for PCR and clean-up are described in Supplementary Table 1. Clean PCR products were then quantified using Nanodrop ND-1000 spectrophotometer, and pooled together in equimolar ratios. 60 µL of this library was further cleaned with a QIAquick Gel Extraction Kit (Qiagen) according to the manufacturer's instructions. The resulting library was quantified on a Qubit 3.0 Fluorometer (Thermo Scientific), diluted to 4 pM and sequenced on a MiSeq platform (Illumina, San Diego, California) using V2 chemistry with 2×150 cycles to obtain paired-end reads for bacteria, and 1×300 cycles for fungi.

498 ***Bioinformatics pipeline***

499 Merging of bacterial paired-end reads and stringent quality-filtering (*fastq_maxdiffs* 1, *fastq_maxee*
500 0.05, and max length 200 bp for fungal reads) were performed with VSEARCH v2.3.4[67]. Non-target
501 regions were removed with a custom *awk* script for bacterial reads, and with the ShortRead R library[68]
502 for fungal reads, before 97% *de novo* OTU clustering using VSEARCH. Chimeras were removed
503 with UCHIME and the GOLD or UNITE v7 databases[69–71] OTUs that were abundant in the technical
504 controls (>5%) were removed, alike in Ref. [16,18]. PyNAST, FastTree, the RDP naïve Bayesian
505 classifier and Greengenes 13.8 or UNITE v7 databases were used in QIIME v1.9.1[72–76] to obtain
506 OTUs taxonomy, filtering out OTUs present in less than 10% of the samples to exclude highly-
507 variable OTUs that may artificially inflate the number of differentially-abundant OTUs (adapted from
508 Ref. [77], see also Ref. [18]). α-diversity metrics (abundance-based coverage estimator ACE) for both
509 bacteria and fungi were computed using QIIME from abundance tables, both derived by averaging
510 100 rarefactions at 5000 sequences depth to minimize loss of samples while ensuring a coverage
511 judged sufficient based on α-diversity rarefaction curves (Extended Data Figures 2 and 10). One
512 sample (ST, day 1) yielded fewer than 5000 high-quality 16S sequences and was excluded from
513 rarefaction-based analyses, while one other sample (ST, day 15) as well as all three pre-incubation
514 permafrost samples did not yield any ITS sequences.

515

516 ***Phospholipid fatty acids (PLFA) extraction***

517 The relative abundance of fungal and bacterial biomarkers in the samples was assessed with the PLFA
518 technique[78], 1, 30 and 161 days after soil transfer. Lipids were extracted from 1.5 g of lyophilised soil
519 with a solution of chloroform, methanol and phosphate buffer (1:2:0.8 volume), and then separated
520 into neutral, glyco-, and phospholipids on silica solid phase extraction cartridges (Supelco, Merck,
521 Darmstadt, Germany). The phospholipids were subsequently trans-esterified in fatty acid methyl
522 esters using 1 mL of 0.2 M methanolic KOH, and detected by gas chromatography (Varian CP3800,

523 Agilent, Santa Clara, USA). Methyl nonadecanoate (19:0) was used as an internal standard and PLFA
524 biomarkers were identified as fungal or bacterial following standard notation[79–82] with reference to
525 commercial standards (Supelco).
526
527 ***Reproduced incubation***
528 In an additional incubation experiment, we tested whether we could generalize our findings by
529 introducing arctic active layer soils as sources of exogenous microorganisms into our Yedoma
530 permafrost as well as in other permafrost soils. For the latter we used different Holocene permafrost
531 soils, because microbial communities in Yedoma permafrost deposits from the Upper Pleistocene may
532 be particularly limited due to their old age. Details on the soils and the incubation conditions are
533 found in Supplementary Methods. Briefly, Yedoma permafrost was inoculated with the three different
534 arctic active layers from the Holocene soils as well as with the donor soil used in the main experiment,
535 to test whether the observed effects of soil transfer on CO_2 production occur with active layer soils
536 (Extended Data Figure 8a). Additionally, the three Holocene permafrost soils, ranging from 1 to 12%
537 organic matter content, were inoculated with our donor soil, to test whether CO_2 production in other
538 permafrost soils responded to coalescence with a functionally diverse microbial community
539 (Extended Data Figure 8b). We incubated *c*. 20g FW of these soils in the dark at 10°C for 389 days,
540 measuring headspace CO_2 concentrations at intervals in a similar manner as in our main experiment
541 (see Supplementary Methods).
542
543 ***Statistical analyses***
544 Aerobic CO_2 production rates were obtained from the measurements made on the harvest date, except
545 for the first harvest (day 2 instead of 1, Extended Data Figure 9). The effects of ST and time on
546 aerobic CO_2 production rates, cumulative CO_2 production (Extended Data Figure 6), soil chemistry,
547 PLFA marker groups, bacterial and fungal α-diversity, and gene abundances were tested using two-

548 way ANOVA, and pairwise comparisons were computed when relevant using the *emmeans* package[83]
549 with Holm adjustment for family-wise error rate. Data transformation was used when necessary to
550 meet homoscedasticity assumptions (Extended Data Figure 3). When the ANOVA assumptions could
551 not be met, non-parametric alternatives were used (Kruskal-Wallis test and Dunn's test, DIN, NH_4^+).
552 The tests excluded ST for NO_3^-+NO_2^-, which was irrelevant since all control sample values were
553 below detection limit. The effects of ST and time on bacterial and fungal community composition
554 were tested using two-way ANOVA on negative-binomial generalized linear models fitted for each
555 OTU (*manyglm* in *mvabund* package[84,85]). Differential abundance of OTUs between treatments for
556 each harvest was assessed using DESeq2[86,87] negative-binomial Wald test on non-rarefied reads in
557 QIIME with Benjamini-Hochberg false discovery rate control. The phylum- and/or class- distribution
558 of differentially abundant OTUs was deemed consistent enough across time points to present only the
559 OTUs changing over the whole incubation in Figure 1 (Extended Data Figures 2 and 10). The
560 proportions of reads belonging to OTUs that were differentially abundant between treatments, as well
561 as those unaffected and those occurring only in either control or ST samples were derived from the
562 rarefied OTU table (Extended Data Figures 2 and 10). Bacterial OTUs able to carry out nitrification
563 were identified based on their assigned taxonomy, which included members of phylum *Nitrospira*
564 and the family *Nitrosomonadaceae*. No other taxa known as ammonia-oxidising bacteria were
565 found[88–90].
566
567 We estimated the relative importance of bacterial community composition, diversity, nitrification
568 potential, microbial biomass, and soil chemistry in explaining the differences in CO_2 production rates
569 between control and ST samples (i.e. de-trended CO_2 production rates: divided by the average within
570 the respective date's values) with RandomForest and multiple linear regressions. Fungal relative
571 abundances and PLFA biomass data, for which fewer dates had been analysed, were excluded to retain
572 as many samples as possible, variables were scaled and centered and we attributed a 0 value to all

values below detection limit to avoid missing values when necessary (i.e. for nitrate + nitrite and *amoA* genes). Altogether, relative abundances of bacterial taxa, proxies of bacterial biomass, *amoA* gene abundances, alpha-diversity and soil chemistry variables amounted up to 47 variables for 29 samples (Extended Data Figure 7). We compared partial-least squares regression and RandomForest using the *caret* package[91] as both methods are suited to having more parameters than observations and can tease out highly collinear variables. RandomForest yielded slightly better MAE, RMSE and pseudo-R^2, thus we used the interpretation phase output of Variable Selection using Random Forests regression (VSURF[92–94]), using default parameters (*mtry* = p/3, 2000 and 25 forests for the thresholding and interpretation phases, respectively). We further used multiple linear regressions of de-trended CO_2 production rates, using either the four variables selected by VSURF ("community-function"), the microbial biomass variables (microbial biomass-C, 16S rRNA gene copy number), the soil chemistry variables (TDC, DIN, ammonium, nitrate + nitrite) or combinations thereof to compare their explanatory power (Table 1).

All analyses were performed using R v3.6.1[95], unless specified otherwise.

Data availability

Sequence data supporting the findings of this study have been deposited at ENA under the project number PRJEB29467 at https://www.ebi.ac.uk/ena/browser/view/PRJEB29467. Processed data files supporting the findings are found at figshare (doi:10.6084/m9.figshare.7713308).

Code availability

Scripts used to produce the figures and tables presented here are found at figshare (doi:10.6084/m9.figshare.7713308). The bioinformatics and analysis pipeline used to reproduce our findings is found at https://bitbucket.org/smonteux/functional_limitations/.

598 **References only in Methods**

599 46. Douglas, T. A. *et al.* Biogeochemical and geocryological characteristics of wedge and
600 thermokarst-cave ice in the CRREL permafrost tunnel, Alaska. *Permafr. Periglac. Process.* **22**, 120–
601 128 (2011).
602 47. Long, A. & Péwé, T. L. Radiocarbon dating by high-sensitivity liquid scintillation counting
603 of wood from the Fox permafrost tunnel near Fairbanks, Alaska. *Permafr. Periglac. Process.* **7**,
604 281–285 (1996).
605 48. Hamilton, T. D., Craig, J. L. & Sellmann, P. V. The Fox permafrost tunnel: A late Quaternary
606 geologic record in central Alaska. *GSA Bull.* **100**, 948–969 (1988).
607 49. Shur, Y., French, H. M., Bray, M. T. & Anderson, D. A. Syngenetic permafrost growth:
608 cryostratigraphic observations from the CRREL tunnel near Fairbanks, Alaska. *Permafr. Periglac.*
609 *Process.* **15**, 339–347 (2004).
610 50. Howard, M. M., Bell, T. H. & Kao-Kniffin, J. Soil microbiome transfer method affects
611 microbiome composition, including dominant microorganisms, in a novel environment. *FEMS*
612 *Microbiol. Lett.* **364**, fnx092 (2017).
613 51. Patra, A. K. *et al.* Effects of grazing on microbial functional groups involved in soil N
614 dynamics. *Ecol. Monogr.* **75**, 65–80 (2005).
615 52. Fontaine, S. *et al.* Fungi mediate long term sequestration of carbon and nitrogen in soil
616 through their priming effect. *Soil Biol. Biochem.* **43**, 86–96 (2011).
617 53. Elberling, B. *et al.* Long-term CO2 production following permafrost thaw. *Nat. Clim.*
618 *Change* **3**, 890–894 (2013).
619 54. Walz, J., Knoblauch, C., Böhme, L. & Pfeiffer, E.-M. Regulation of soil organic matter
620 decomposition in permafrost-affected Siberian tundra soils - Impact of oxygen availability, freezing
621 and thawing, temperature, and labile organic matter. *Soil Biol. Biochem.* **110**, 34–43 (2017).

622 55. Weedon, J. T. *et al.* Temperature sensitivity of peatland C and N cycling: Does substrate
623 supply play a role? *Soil Biol. Biochem.* **61**, 109–120 (2013).
624 56. Ping, C. L. Soil Temperature Profiles of Two Alaskan Soils 1. *Soil Sci. Soc. Am. J.* **51**, 1010–
625 1018 (1987).
626 57. D'Amico, S. *et al.* Psychrophilic microorganisms: challenges for life. *EMBO Rep.* **7**, 385–
627 389 (2006).
628 58. Vance, E. D., Brookes, P. C. & Jenkinson, D. S. An extraction method for measuring soil
629 microbial biomass C. *Soil Biol. Biochem.* **19**, 703–707 (1987).
630 59. Wu, J., Joergensen, R. G., Pommerening, B., Chaussod, R. & Brookes, P. C. Measurement
631 of soil microbial biomass C by fumigation-extraction—an automated procedure. *Soil Biol. Biochem.*
632 **22**, 1167–1169 (1990).
633 60. Rotthauwe, J. H., Witzel, K. P. & Liesack, W. The ammonia monooxygenase structural gene
634 amoA as a functional marker: molecular fine-scale analysis of natural ammonia-oxidizing
635 populations. *Appl. Environ. Microbiol.* **63**, 4704–4712 (1997).
636 61. Tourna, M., Freitag, T. E., Nicol, G. W. & Prosser, J. I. Growth, activity and temperature
637 responses of ammonia-oxidizing archaea and bacteria in soil microcosms. *Environ. Microbiol.* **10**,
638 1357–1364 (2008).
639 62. Fowler, S. J., Palomo, A., Dechesne, A., Mines, P. D. & Smets, B. F. Comammox Nitrospira
640 are abundant ammonia oxidizers in diverse groundwater-fed rapid sand filter communities. *Environ.*
641 *Microbiol.* **20**, 1002–1015 (2018).
642 63. Pjevac, P. *et al.* AmoA-Targeted Polymerase Chain Reaction Primers for the Specific
643 Detection and Quantification of Comammox Nitrospira in the Environment. *Front. Microbiol.* **8**,
644 1508 (2017).

64. Muyzer, G., Waal, E. C. de & Uitterlinden, A. G. Profiling of complex microbial populations by denaturing gradient gel electrophoresis analysis of polymerase chain reaction-amplified genes coding for 16S rRNA. *Appl. Environ. Microbiol.* **59**, 695–700 (1993).

65. Bartram, A. K., Lynch, M. D. J., Stearns, J. C., Moreno-Hagelsieb, G. & Neufeld, J. D. Generation of Multimillion-Sequence 16S rRNA Gene Libraries from Complex Microbial Communities by Assembling Paired-End Illumina Reads. *Appl. Environ. Microbiol.* **77**, 3846–3852 (2011).

66. Smith, D. P. & Peay, K. G. Sequence Depth, Not PCR Replication, Improves Ecological Inference from Next Generation DNA Sequencing. *PLOS ONE* **9**, e90234 (2014).

67. Rognes, T., Flouri, T., Nichols, B., Quince, C. & Mahé, F. VSEARCH: a versatile open source tool for metagenomics. *PeerJ* **4**, e2584 (2016).

68. Morgan, M. *et al.* ShortRead: a bioconductor package for input, quality assessment and exploration of high-throughput sequence data. *Bioinformatics* **25**, 2607–2608 (2009).

69. Edgar, R. C., Haas, B. J., Clemente, J. C., Quince, C. & Knight, R. UCHIME improves sensitivity and speed of chimera detection. *Bioinformatics* **27**, 2194–2200 (2011).

70. Haas, B. J. *et al.* Chimeric 16S rRNA sequence formation and detection in Sanger and 454-pyrosequenced PCR amplicons. *Genome Res.* **21**, 494–504 (2011).

71. Kõljalg, U. *et al.* Towards a unified paradigm for sequence-based identification of fungi. *Mol. Ecol.* **22**, 5271–5277 (2013).

72. Caporaso, J. G. *et al.* QIIME allows analysis of high-throughput community sequencing data. *Nat. Methods* **7**, 335–336 (2010).

73. Price, M. N., Dehal, P. S. & Arkin, A. P. FastTree 2 – Approximately Maximum-Likelihood Trees for Large Alignments. *PLoS ONE* **5**, e9490 (2010).

74. Caporaso, J. G. *et al.* PyNAST: a flexible tool for aligning sequences to a template alignment. *Bioinformatics* **26**, 266–267 (2010).

75. McDonald, D. *et al.* An improved Greengenes taxonomy with explicit ranks for ecological and evolutionary analyses of bacteria and archaea. *ISME J.* **6**, 610–618 (2012).

76. Wang, Q., Garrity, G. M., Tiedje, J. M. & Cole, J. R. Naive Bayesian Classifier for Rapid Assignment of rRNA Sequences into the New Bacterial Taxonomy. *Appl. Environ. Microbiol.* **73**, 5261–5267 (2007).

77. Lagkouvardos, I., Fischer, S., Kumar, N. & Clavel, T. Rhea: a transparent and modular R pipeline for microbial profiling based on 16S rRNA gene amplicons. *PeerJ* **5**, e2836 (2017).

78. White, D. C., Davis, W. M., Nickels, J. S., King, J. D. & Bobbie, R. J. Determination of the sedimentary microbial biomass by extractible lipid phosphate. *Oecologia* **40**, 51–62 (1979).

79. Olsson, P. A., Bååth, E., Jakobsen, I. & Söderström, B. The use of phospholipid and neutral lipid fatty acids to estimate biomass of arbuscular mycorrhizal fungi in soil. *Mycol. Res.* **99**, 623–629 (1995).

80. Ruess, L. & Chamberlain, P. M. The fat that matters: Soil food web analysis using fatty acids and their carbon stable isotope signature. *Soil Biol. Biochem.* **42**, 1898–1910 (2010).

81. Zelles, L. Fatty acid patterns of phospholipids and lipopolysaccharides in the characterisation of microbial communities in soil: a review. *Biol. Fertil. Soils* **29**, 111–129 (1999).

82. Frostegård, A. & Bååth, E. The use of phospholipid fatty acid analysis to estimate bacterial and fungal biomass in soil. *Biol. Fertil. Soils* **22**, 59–65 (1996).

83. Lenth, R. Least-Squares Means: The R Package lsmeans. *J. Stat. Softw.* **69**, 1–33 (2016).

84. Wang, Y., Naumann, U., Wright, S. T. & Warton, D. I. mvabund– an R package for model-based analysis of multivariate abundance data. *Methods Ecol. Evol.* **3**, 471–474 (2012).

85. Warton, D. I., Wright, S. T. & Wang, Y. Distance-based multivariate analyses confound location and dispersion effects. *Methods Ecol. Evol.* **3**, 89–101 (2012).

86. Love, M. I., Huber, W. & Anders, S. Moderated estimation of fold change and dispersion for RNA-seq data with DESeq2. *Genome Biol.* **15**, 550 (2014).

695 87. McMurdie, P. J. & Holmes, S. Waste Not, Want Not: Why Rarefying Microbiome Data Is
696 Inadmissible. *PLoS Comput Biol* **10**, e1003531 (2014).
697 88. Pinto, A. J. *et al.* Metagenomic Evidence for the Presence of Comammox *Nitrospira* -Like
698 Bacteria in a Drinking Water System. *mSphere* **1**, e00054-15 (2016).
699 89. Kozlowski, J. A., Kits, K. D. & Stein, L. Y. Comparison of Nitrogen Oxide Metabolism
700 among Diverse Ammonia-Oxidizing Bacteria. *Front. Microbiol.* **7**, 1090 (2016).
701 90. Kits, K. D. *et al.* Kinetic analysis of a complete nitrifier reveals an oligotrophic lifestyle.
702 *Nature* **549**, 269–272 (2017).
703 91. Kuhn, M. *et al. caret: Classification and Regression Training*. (2020).
704 92. Breiman, L. Random Forests. *Mach. Learn.* **45**, 5–32 (2001).
705 93. Hastie, T., Tibshirani, R. & Friedman, J. *The Elements of Statistical Learning: Data Mining,*
706 *Inference, and Prediction, Second Edition*. (Springer-Verlag, 2009).
707 94. Genuer, R., Poggi, J.-M. & Tuleau-Malot, C. VSURF: An R Package for Variable Selection
708 Using Random Forests. *R J.* **7**, 19 (2015).
709 95. R Core Team. R: A Language and Environment for Statistical Computing. (2019).

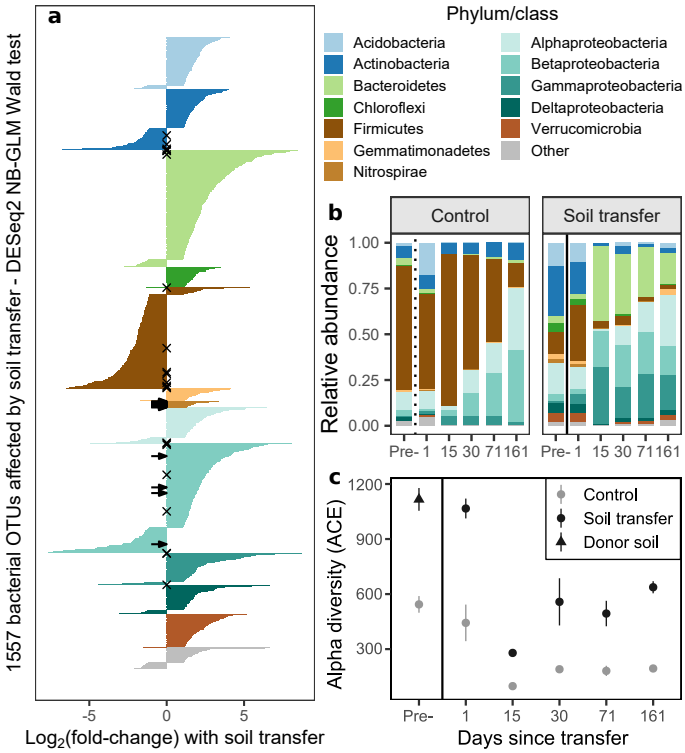

Figure 1: Changes in permafrost bacterial communities with inoculation by soil transfer (ST).
a: Differential abundance of OTUs between ST and control samples over days 1-161 (n=15). Each bar is a significantly changing OTU, a positive fold-change indicates higher relative abundance in ST. Crosses indicate most abundant OTUs (>0.5% rarefied observations) and arrows indicate nitrifiers. **b:** Phylum-/class-level summary of average relative abundances for control and ST samples. **c:** Alpha-diversity (Abundance-based Coverage Estimator) of bacterial communities in control and ST samples (mean ± SE). In **b** and **c**: n=3 except ST, day 1 where n=2; vertical lines separate pre-incubation permafrost (control) and donor soil (left) from incubated samples (right).

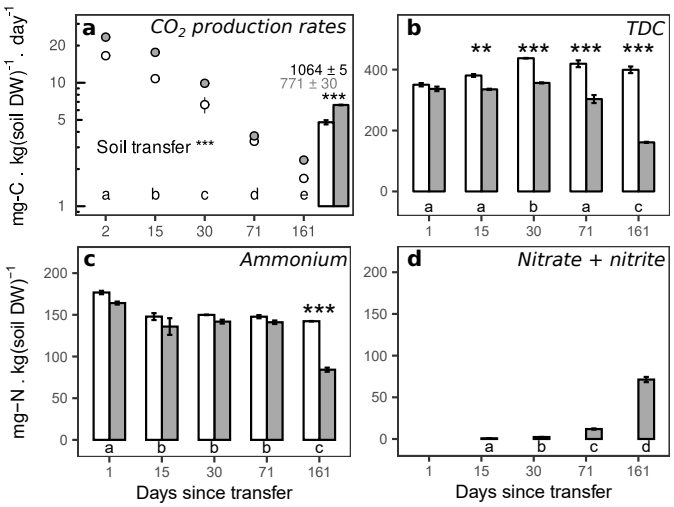

Figure 2: Changes in permafrost carbon and nitrogen fluxes and pools with soil transfer (ST).
a: Daily CO_2 production rates at five dates (circles) and averaged over 161 days (bars). Numbers indicate cumulative CO_2 production after 161 days. **b:** Total dissolved carbon content. **c:** Ammonium content. **d:** Nitrate and nitrite content. **(a-d):** white colour indicates control, grey colour ST (means ± SE, n=3). Asterisks denote significant ST effect for averaged rates (**a**) or within a day (significant 'ST x time' interaction; **b-c**). Letters indicate significant differences between days (main effect); ** P ≤ 0.01; *** P ≤ 0.001. Values in (**d**) for control (day 1-161) and ST (day 1) are below detection limit.

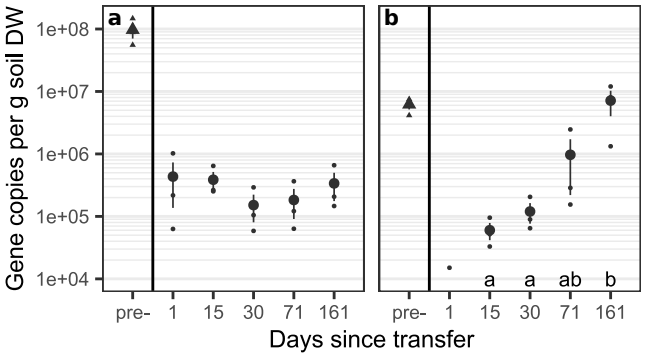

Figure 3: Abundances of (a) archaeal and (b) bacterial *amoA* genes in permafrost inoculated by soil transfer (ST) over 161 days. Abundances of *amoA* genes for control samples (all days, **a-b**), as well as two ST samples for bacteria (day 1, **b**) were below detection limit. Small symbols indicate values for individual samples (average of two technical replicates), large symbols indicate means (n=3), error-bars indicate standard-error of the mean (n=3) and different lower-case letters indicate significant differences between days (excluding pre-incubation). The black vertical lines separate pre-incubation donor soil (left, triangles) from incubated samples (right, circles).

Extended Data Figure 1: **Summary of initial chemistry of the permafrost used for incubation and of the topsoil used for the soil transfer treatment (top, mean ± SE, n = 3) and estimated average C and N content of incubated jars for each treatment (bottom).**

Initial soil chemistry

	Permafrost homogenized	Donor soil	Two-sided Welch's t (*P*)
%C	3.05 ± 0.02	3.13 ± 0.20†	$t_{2.098}$ = -0.493 (*0.669*)
%N	0.24 ± 0.00	0.32 ± 0.02†	$t_{2.114}$ = -4.801* (*0.037*)
C/N	12.50 ± 0.07	9.77 ± 0.03†	$t_{2.843}$ = 40.406* ($<10^{-4}$)
TDC (mgC.kg soil DW^{-1})	350.30 ± 6.65	39.10 ± 16.77	$t_{2.613}$ = 21.124* (5.10^{-4})
DIN (mgN.kg soil DW^{-1})	176.77 ± 2.47	126.68 ± 5.44	$t_{2.793}$ = 10.273* (*0.003*)
pH	7.10 ± 0.00	6.30 ± 0.00	ND

†: data from Ref. 27 (Fontaine *et al*. 2007; doi:10.1038/nature06275). *: Welch's test P < 0.05, pH values could not be tested due to virtually inexistent variance (replicate measurements were identical).

Estimated incubation jars content

		Control	Soil transfer
19.5g DW Permafrost	**C (mg)**	594.750	594.750
	of which TDC (mg-C)	6.831	6.831
	N (mg)	46.800	46.800
	of which DIN (mg-N)	3.447	3.447
0.5g DW Treatment (Permafrost for Control, Donor soil for ST)	**C (mg)**	15.250	15.650
	of which TDC (mg-C)	0.175	0.020
	N (mg)	1.200	1.600
	of which DIN (mg-N)	0.088	0.063
20g DW Total	**C (mg)**	610.000	610.400
	of which TDC (mg-C)	7.006	6.851
	N (mg)	48.000	48.400
	of which DIN (mg-N)	3.535	3.510

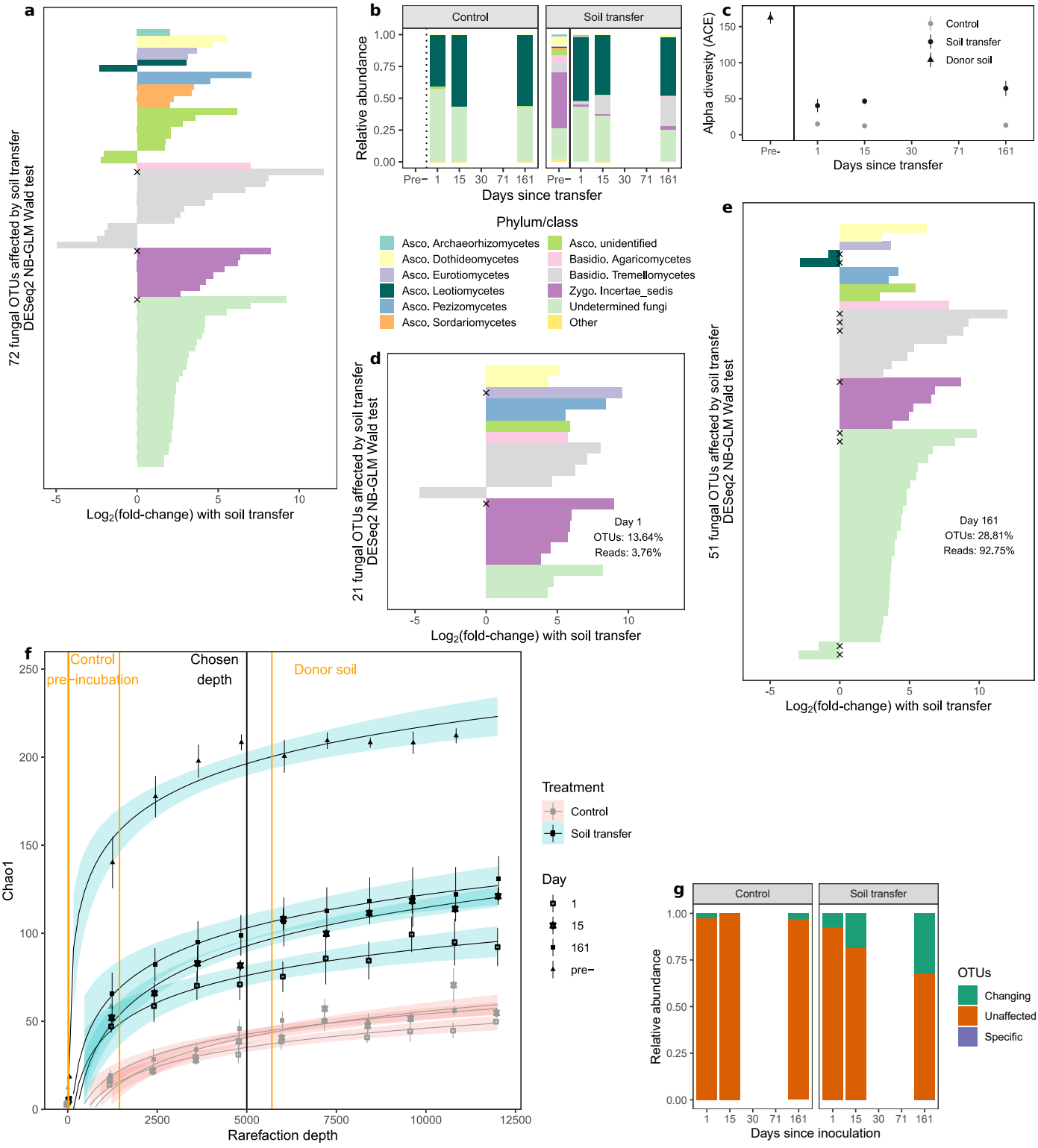

Extended Data Figure 2: Changes in Yedoma permafrost fungal communities with soil transfer (ST).
a: Differential abundance of OTUs between ST and control samples over three sampling times (days 1, 15, 161, n=9 for control soils, n=8 for ST soils); each bar is a significantly changing OTU, arranged by decreasing fold-change within a class; positive fold-change indicates higher relative abundance in ST samples; crosses indicate most abundant OTUs (>0.5% rarefied observations).
b: Phylum-/class-level summary of average relative abundances for control and ST samples.
c: Alpha diversity (Abundance-based Coverage Estimator) of fungal communities in control and ST samples; means ± SE.
d-e: Differential abundance of OTUs between ST and control samples after 1 (**d**) and 161 (**e**) days of incubation. Due to one ST sample failing sequencing, the test could not be carried out for day 15. OTU percentage denotes the proportion of OTUs with significantly different abundance among those present at the respective date; reads percentage represents the proportion of rarefied reads these OTUs represent at the respective date.
f: Fungal alpha-diversity response to rarefaction depth in control and ST samples over the 161 days incubation, based on 10 rarefactions at 12 evenly-spaced depths between 10 and 12000 reads per sample (means ± SE, n=2-3).
g: Relative abundance along the 161 days incubation of the OTUs in control and ST samples which were overall affected by ST (Changing, see panel **a**), not affected by ST (Unaffected) or present only in either control or ST samples (Specific). The proportion of reads belonging to Changing OTUs differ from those in panels (**d-e**) because they refer to the test carried over the entire incubation period (as in panel **a**) rather than within each date.
(b-c, g): n=3 except for ST, day 15 where n=2. Vertical lines in (**b-c**) separate the pre-incubation donor soil (left) from the incubated samples (right); no fungal sequences could be obtained in pre-incubation permafrost.

Extended Data Figure 3: Soil transfer (ST) and time effects on permafrost microbial communities, soil chemistry, microbial biomass and functional genes (ANOVA). 'Δ-Day 1' is the post-hoc pairwise comparison between control and ST samples at Day 1, in cases when the interaction is significant ($P < 0.05$), with Holm P-value adjustment for multiple comparisons. Bold text denotes significant p-values ($P < 0.05$); n = 3, excepted for ManyGLM ANOVAs where n = 2 for 'ST – day 1' (Bacteria) and 'ST – day 15' (Fungi).

	Soil transfer			Time			Soil transfer × Time		
Microbial community (ManyGLM)	**Dev**	**df**	***P***	**Dev**	**df**	***P***	**Dev**	**df**	***P***
Bacteria (4768 OTUs)	13526	1	**0.001**	26098	4	**0.001**	3420	4	**0.002**
Fungi (280 OTUs)	848	1	**0.002**	687	2	**0.002**	149	2	**0.022**

	Soil transfer			Time			Soil transfer × Time			Δ-Day 1	
Variable	**F-value**	**df**	***P***	**F-value**	**df**	***P***	**F-value**	**df**	***P***	**t.ratio**	p_{Holm}
Microbial α-diversity											
Bacterial α-diversity (ACE)*	106.83	1	**$<10^{-4}$**	20.83	4	**$<10^{-4}$**	0.19	4	0.943		
Fungal α-diversity (ACE)*	112.99	1	**$<10^{-4}$**	1.09	2	0.369	2.48	2	0.129		
Biogeochemistry											
CO_2 production rates*	72.67	1	**$<10^{-4}$**	451.93	4	**$<10^{-4}$**	2.63	4	0.065		
Dissolved C*	588.03	1	**$<10^{-4}$**	128.90	4	**$<10^{-4}$**	135.38	4	**$<10^{-4}$**	1.35	0.815
Dissolved inorganic N ‡	0.16‡	1	0.694	15.15‡	4	**0.004**	23.63‡	9	**0.005**	-0.42‡	1.000
NH_4^+*	74.23	1	**$<10^{-4}$**	60.24	4	**$<10^{-4}$**	25.21	9	**$<10^{-4}$**	1.87	0.724
$NO_3^{2-} + NO_2^-$ *†§	NA†§			1064.10	3§	**$<10^{-4}$**	NA†§				
Microbial biomass and functions											
Microbial biomass C*	0.04	1	0.846	10.56	4	**$<10^{-4}$**	0.93	4	0.465		
Total PLFA	1.18	1	0.299	17.51	2	**3.10^{-4}**	1.28	2	0.312		
Bacterial PLFA*	0.97	1	0.343	27.42	2	**$<10^{-4}$**	0.17	2	0.849		
Fungal PLFA	32.96	1	**$<10^{-4}$**	26.48	2	**$<10^{-4}$**	4.30	2	**0.039**	1.22	0.733
Protozoan PLFA*	1.45	1	0.252	0.25	2	0.780	0.71	2	0.513		
Fungi : Bacteria PLFA ratio*	11.45	1	**0.005**	17.08	2	**3.10^{-4}**	0.16	2	0.858		
16S rRNA gene copy number *	9.29‡	1	**0.002**	12.99‡	4	**0.011**	27.31‡	9	**0.001**	-0.56‡	0.289
Archaeal *amoA* gene copy number †	NA†			0.54	4	0.710	NA†				
Bacterial amoA gene copy number **†§	NA†§			6.99	3†	**0.013**	NA†§				

*: log-transformation; **: square-root transformation; ‡ Kruskal χ^2 or Dunn Z; †: all Control soils- and §: day 1 samples- excluded from analysis because of values below detection limit

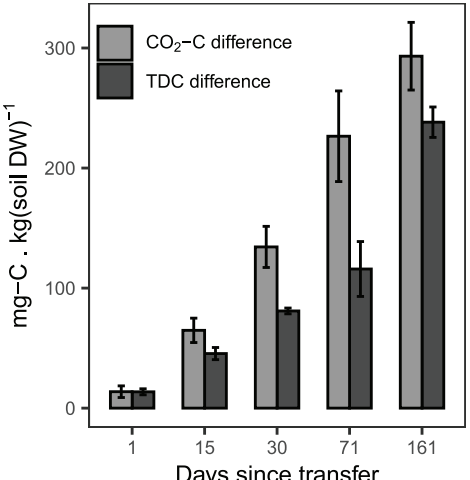

Extended Data Figure 4: Absolute differences in cumulative CO_2 production (CO_2-C) and in total dissolved carbon (TDC) between control and Soil transfer samples over 161 days of incubation. Means ± SE (n=3).

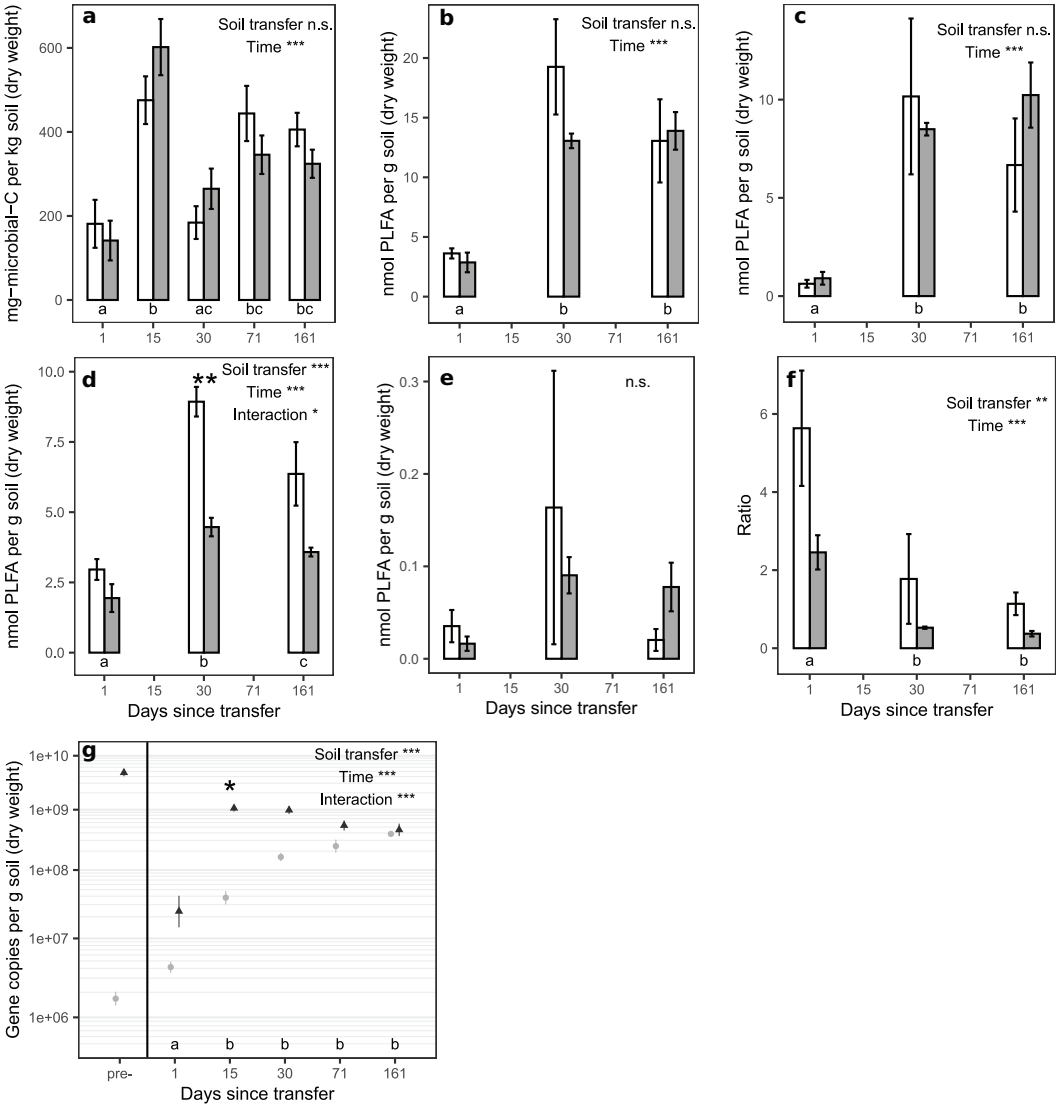

Extended Data Figure 5: Microbial proxies of microbial biomass in Yedoma permafrost with and without soil transfer (ST).
a: Microbial biomass C; **b:** total PLFA; **c:** Bacterial PLFA; **d:** Fungal PLFA; **e:** Protozoan PLFA; **f:** Fungal : bacterial PLFA ratio; **g:** 16S rRNA gene copy number. Light bars and symbols are control samples, dark bars and symbols are ST. (**g**): Vertical line separates pre-incubation permafrost (control) and donor soil (left; "pre-") from incubated samples (right), ANOVA and pairwise differences are based on incubated samples only. Asterisks over bars denote significant differences with ST at a given day (when the ST x time interaction is significant), letters indicate significant differences between days (main effect); n.s. = non-significant ($P > 0.05$), * $P \leq 0.05$; ** $P \leq 0.01$; *** $P \leq 0.001$. Means ± SE (n=3).

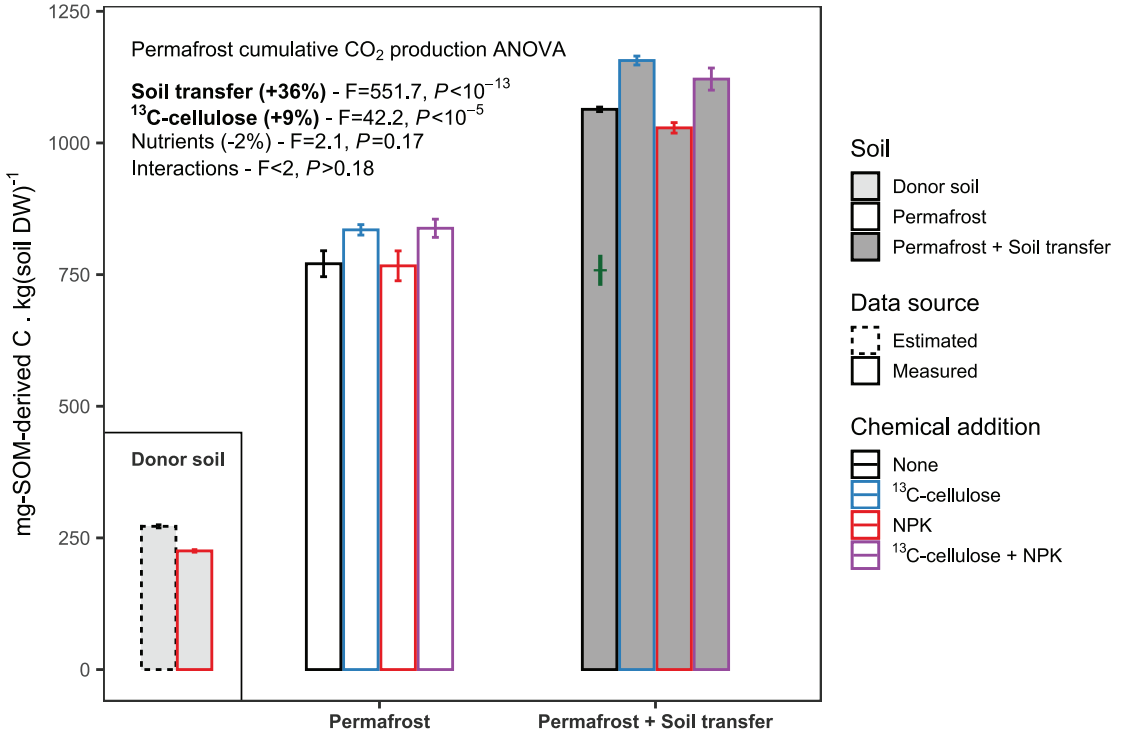

Extended Data Figure 6: Cumulative soil organic matter (SOM)-derived aerobic CO_2 production after 161 days incubation of permafrost with or without Soil transfer (bars with black outline correspond to values in Fig. 2a), and with addition of nutrients (NPK), ^{13}C-cellulose and their combination. CO_2 production of the donor soil is shown in the inset as measured when incubated with nutrients (solid red outline), and estimated when incubated without nutrients using data from Ref. 52 (Fontaine *et al.*, 2011, doi:10.1016/j.soilbio.2010.09.017, dashed black outline). The green "+" symbol in the "Permafrost + Soil transfer" black outline bar represents the expected effect of Soil transfer assuming no biotic interactions (i.e. 97.5% CO_2 production of control soil + 2.5% CO_2 production of donor soil without NPK). ANOVA statistics and effect sizes shown are derived from permafrost soils only, means ± SE (n=3).

Extended Data Figure 7: RandomForests variable selection (VSURF) on bacterial phyla relative abundance, bacterial and archaeal *amoA* and 16S genes abundance, alpha-diversity, soil chemistry and microbial biomass-C to select the variables explaining best the difference in detrended CO_2 production rates. Importance is non-normalized % Increase in Mean Squared Error of a tree when the variable is randomly permuted in out-of-bag (OOB) samples (i.e. a higher value indicates a higher importance), variables are ranked by decreasing importance. $OOB_{interpretation}$ is the out-of-bag error of the nested forests (i.e. grown using this variable as well as all variables with greater importance), the VSURF algorithm selects variables leading to the lowest $OOB_{interpretation}$ score. Variables in grey were considered uninformative at the thresholding phase, variables in bold were selected at the interpretation phase and are termed "Community + function" in Table 1. Variables in bold and italics are included in the multiple linear regression models presented in Table 1.

Variable	Mean importance	SD importance	$OOB_{interpretation}$	Model group
Bacterial *amoA* gene (AOB)	**0.009811**	**0.000515**	**0.016329**	**Community + function**
Archaeal *amoA* gene (AOA)	**0.007038**	**0.000457**	**0.012572**	**Community + function**
Bacteroidetes	**0.003779**	**0.000304**	**0.013552**	**Community + function**
WS3	**0.002752**	**0.000266**	**0.012391**	**Community + function**
Nitrate + nitrite	0.002119	0.000233	0.012701	Chemistry
Spirochaetes	0.002084	0.000216	0.013940	
Planctomycetes	0.001939	0.000233	0.013903	
Fibrobacteres	0.001726	0.000218	0.014243	
Alpha diversity ACE	0.001522	0.000164	0.014272	
16S rRNA gene abundance	0.000720	0.000122	0.014329	Microbial biomass
Actinobacteria	0.000690	0.000119	0.015108	
Firmicutes	0.000641	0.000146	0.015680	
Gammaproteobacteria	0.000564	0.000134	0.015961	
TDC	0.000368	0.000130	0.015852	Chemistry
Chlorobi	0.000250	0.000074	0.016349	
Tenericutes	0.000244	0.000051	0.016179	
Cyanobacteria	0.000221	0.000067	0.015742	
Nitrospirae	0.000166	0.000065	0.015900	
TM7	0.000108	0.000073	0.015884	
Verrucomicrobia	0.000094	0.000089	0.015905	
Elusimicrobia	0.000067	0.000036	0.016167	
Betaproteobacteria	0.000057	0.000059	0.016027	
TM6	0.000056	0.000042	0.016109	
DIN	0.000051	0.000050	0.016484	Chemistry
Ammonium	0.000040	0.000050	0.016463	Chemistry
FCPU426	0.000036	0.000025	0.016352	
WS2	0.000025	0.000037	0.016552	
Chloroflexi	0.000020	0.000059	NA	
Armatimonadetes	0.000016	0.000037	NA	
MVP-21	0.000014	0.000023	NA	
Chlamydiae	0.000014	0.000028	NA	
Alphaproteobacteria	0.000010	0.000070	NA	
GN02	0.000004	0.000016	NA	
WS5	0.000001	0.000013	NA	
BRC1	0.000000	0.000002	NA	
Other phyla	-0.000002	0.000046	NA	
WPS-2	-0.000003	0.000024	NA	
OP3	-0.000005	0.000008	NA	
WS4	-0.000010	0.000014	NA	
FBP	-0.000019	0.000015	NA	
OD1	-0.000029	0.000029	NA	
OP11	-0.000033	0.000019	NA	
AD3	-0.000048	0.000040	NA	
Acidobacteria	-0.000165	0.000081	NA	
Microbial biomass C	-0.000195	0.000051	NA	Microbial biomass
Gemmatimonadetes	-0.000444	0.000069	NA	
Deltaproteobacteria	-0.000732	0.000090	NA	

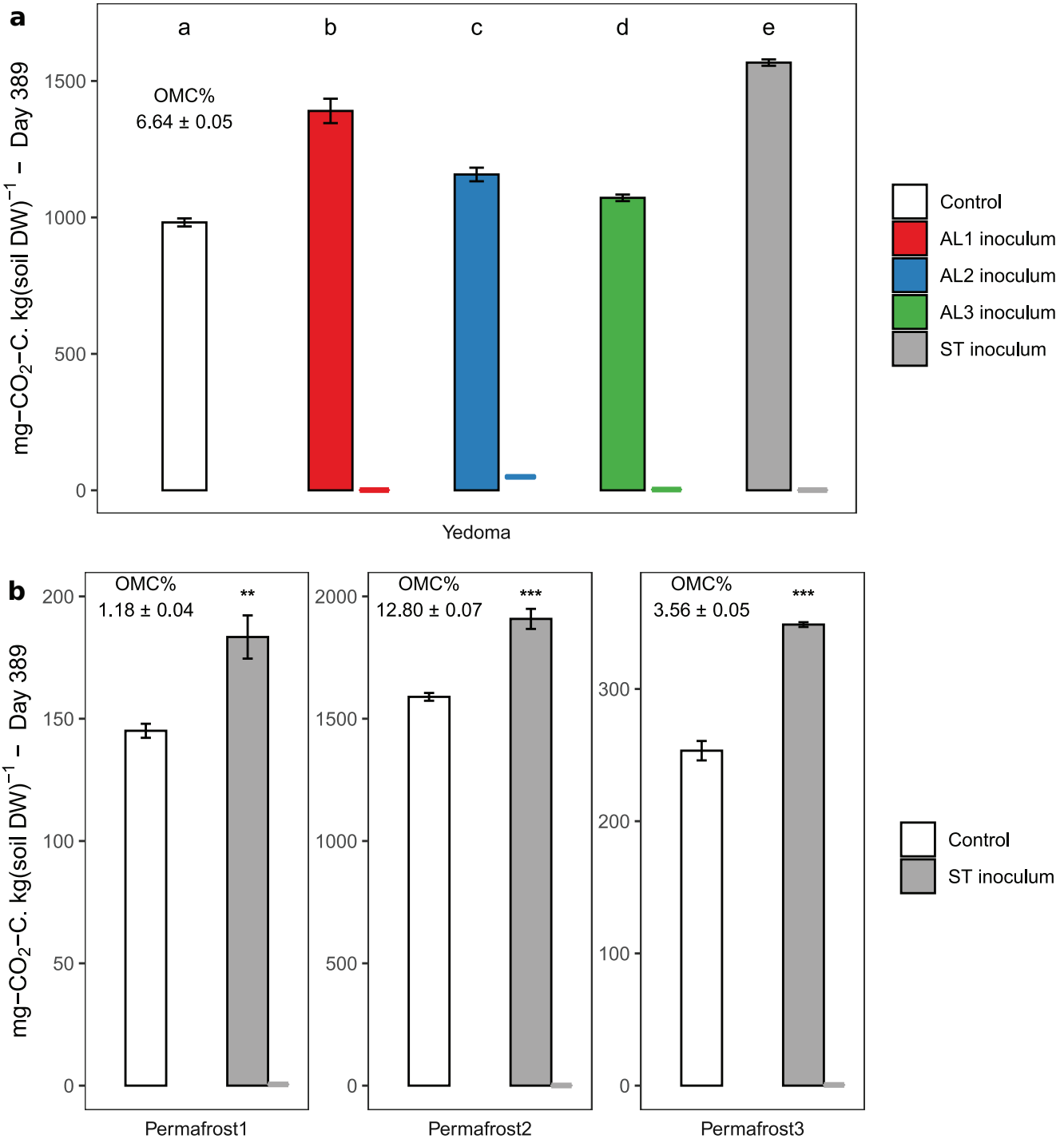

Extended Data Figure 8: Cumulative CO_2 production after 389 days of (a) Yedoma permafrost inoculated with soil suspensions from three Arctic active layer soils and the donor soil used in the main experiment and (b) three other permafrost soils inoculated with donor soil suspension.

a: "Control" and "ST inoculum" reproduce the "Permafrost" and "Soil transfer" described in the main text, except for using a soil suspension instead of solid soil transfer as inoculum, and sterile ddH_2O in controls. AL1, AL2 and AL3 are likewise soil suspension inocula originating from three distinct active layer soils. Different letters denote significant (Holm-adjusted $P < 0.05$) differences between inocula.

b: "Control" for each permafrost type is inoculated with sterile ddH_2O, "ST inoculum" is as in (**a**). Asterisks denote significantly higher values than control, within a soil type (Welch's one-tailed two sample t-test, **: $P < 0.01$; ***: $P < 0.001$).

a-b: Means ± SE, n=4. Coloured and grey error-bars in the lower part denote the quantity of total dissolved carbon (mg-C . g soil DW^{-1}) added with the soil suspensions upon inoculation. OMC%: Organic matter content (determined by loss on ignition at 475°C) in %. A description of the active layer soils used for preparing inoculum suspensions (**a**) and of the permafrost soils inoculated with ST inoculum (**b**) is found in Supplementary Methods.

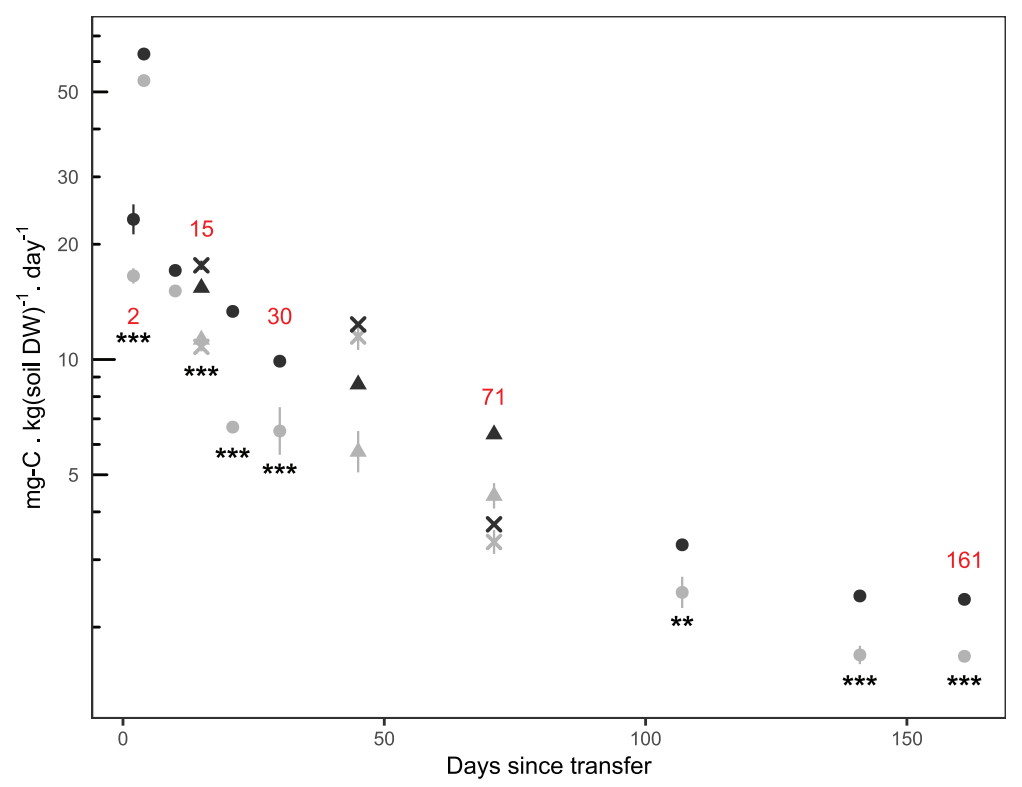

Extended Data Figure 9: Measured and interpolated CO_2 production rates in Yedoma permafrost without (grey) and with soil transfer (black) over the course of 161 days. Circles denote measurements of flasks destructively harvested at day 161, triangles represent rates derived by linear interpolation from these data, used to calculate cumulative CO_2 production. Crosses represent the rates measured at the same dates on the set of flasks destructively harvested at day 71, for comparison. Numbers in red indicate the days of measurements linked to destructive harvests. Means ± SE (n=3), error-bars are shown unless smaller than the plotting symbols, asterisks indicate significant differences between control and ST soils at a given date, for the measured rates (i.e. circles and crosses; **: $P < 0.01$; ***: $P < 0.001$), note the $\log_{10}$ y-axis.

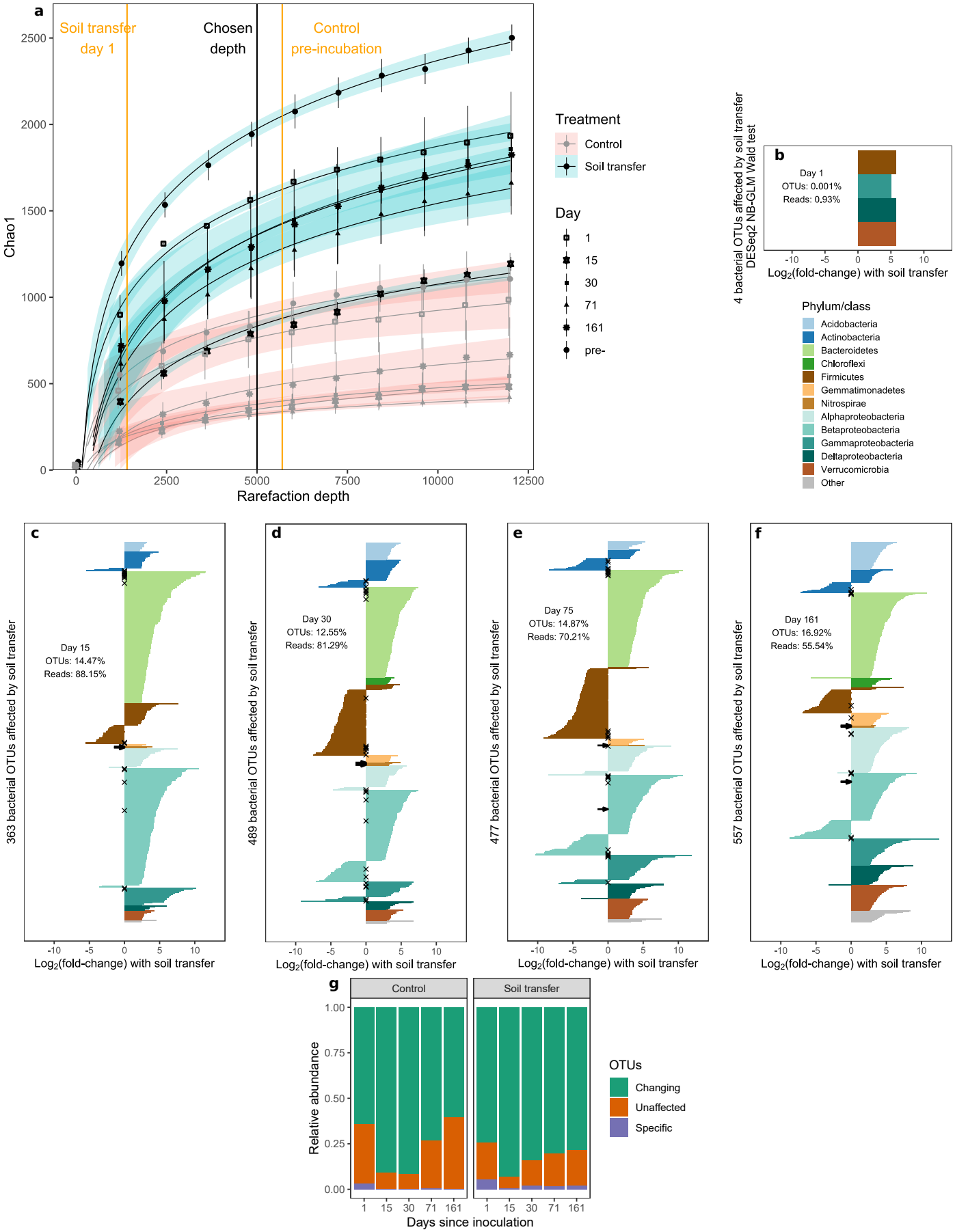

Extended Data Figure 10: Changes in Yedoma permafrost bacterial communities with soil transfer (ST). (a) Bacterial alpha-diversity response to rarefaction depth in control and ST samples over the 161-days incubation, based on 10 rarefactions at 12 evenly-spaced depths between 10 and 12000 reads per sample (means ± SE, n=2-3). **(b-f)** Differential abundance of bacterial OTUs between ST and control samples after **(b)** 1; **(c)** 15; **(d)** 30; **(e)** 75 and **(f)** 161 days of incubation. Each bar is a significantly-changing OTU, arranged by decreasing fold-change within a phylum or class; positive fold-change indicates higher relative abundance in ST samples; crosses indicate the most abundant OTUs (>0.5% rarefied observations); arrows indicate nitrifiers; OTU percentage denotes the proportion of OTUs with significantly changing abundance among those present at the respective date; reads percentage denotes the proportion of (rarefied) reads these OTUs represent at the respective date. **(g)** Relative abundance along the 161-day incubation of the OTUs in control and ST samples which were overall affected by ST (Changing, see Figure 1a), not affected by ST (Unaffected), or present in only either control or ST samples (Specific); the proportion of reads belonging to Changing OTUs differs from those in panels (**b-f**) because they refer to the test carried over the entire incubation period (as in Figure 1a) rather than within each date.

Supplementary Discussion

Potential alternative explanations for observed changes in permafrost carbon and nitrogen fluxes and pools with 2.5% soil transfer

In this section, we discuss potential alternative explanations for the observed appearance of nitrification and the large increase in CO_2 production in permafrost soil, after inoculation with a diverse microbial community by a replacement of 2.5 % (DW basis) of the studied permafrost (Yedoma sediment) with a donor topsoil of known high functional diversity (Soil Transfer; ST; Refs 26-27, 51-52). We present measured data and model outputs that we believe render these four potential alternative explanations unlikely: 1) immediate increase in microbial biomass, 2) introduction of carbon with a higher decomposition rate, 3) relieve of potential nutrient limitation, and 4) priming effect (*sensu* Ref. 94: "the extra decomposition of SOM after addition of easily decomposable organic materials") through addition of labile C and N compounds.

1. Did the "donor" soil cause a transfer of microbial biomass and can such immediate increase in microbial biomass explain the observed increases in nitrification and CO_2 production rates after soil transfer?

No. We did not observe a significant increase in any measured proxies of microbial biomass one day after transfer (K_2SO_4-extractable microbial C, PLFA, 16S rRNA gene copy number, Extended Data Figure 5). The concordant absence of increases across these three different microbial biomass proxies makes it unlikely that the initiation of nitrification and the enhanced CO_2 production rates were caused by (initially) increased microbial biomass by the soil transfer.

2. Was the carbon in the "donor" soil used for soil transfer easier to decompose and could this explain the observed increase in CO_2 production rates?

No. Firstly, the cumulative CO_2 production over 161 days of the donor soil used for soil transfer was about 65% *lower* than that observed in the control permafrost samples (Extended Data Figure 6; Supplementary Methods), despite its already established non-psychrophilic microbial community. Without any biological interaction mechanisms, we would therefore expect that replacing 2.5% of the permafrost soil with donor soil (both *c*. 3% C, Extended Data Figure 1) would *reduce* the overall cumulative CO_2 production by 1.8% compared to pure permafrost soil (green dot in Extended Data Figure 6), instead of the observed 38% *increase*.

Secondly, the total amount of introduced dissolved carbon (TDC) of the donor soil is *smaller* (*c.* 0.02 mg-C per jar added) than in the permafrost sediment (0.175 mg-C per jar removed; Extended Data Figure 1), and although it could potentially be more easily degraded by the Yedoma permafrost microorganisms, the amount is by far not large enough to explain the difference in CO_2 production (*c.* 5.86 mg-C per jar) between the control and soil transfer treatments. Even if we assume that all permafrost and donor TDC is labile and mineralised, the permafrost microorganisms would need to decompose the donor SOC (of both favourable and less-favourable compound composition) at 28 times higher rates than their native C and at 52 times higher rates than the native donor soil microbes in donor soil, if all the remaining increase in CO_2 production would come from mineralization of SOC from the donor soil only. This is equivalent to a SOC mineralization of 38.5% from the 0.5 g DW donor soil (over 161 days), while the estimated cumulative CO_2 production from this donor soil in isolation (Extended Data Figure 6) indicates a SOC mineralization of only 0.74%. We deem it unrealistic that Yedoma microbes would decompose the donor SOC at so much higher rates than the native donor soil community, but not have the same effect in the Yedoma sediment in absence of soil transfer.

Finally, in the incubation experiment carried out to reproduce our findings, microbial communities were manipulated by using a liquid soil suspension rather than soil transfer, introducing smaller amounts of carbon. The addition of 1 mL of donor soil suspension introduced *c*. 0.68 mg-TDC kg soil DW^{-1}, but resulted in an average 585 mg-C kg soil DW^{-1} increase in CO_2 production compared to ddH_2O addition control soils after 389 days ('ST inoculum', Extended Data Figure 8).

We conclude from this that it is highly unlikely that a higher CO_2 production in the donor soil and the replacement of 2.5% of the permafrost soil with this donor soil can explain the observed increase in CO_2 production.

3. Did the donor soil contain more nutrients than the permafrost sediment, and could this have relieved a potential nutrient-limitation in the permafrost soil, explaining the observed difference in CO_2 production rates?

No. CO_2 production could theoretically be constrained by a lack of nitrogen, phosphorus or potassium, which the donor soil could have added upon soil transfer. The nitrogen content of the donor soil was indeed *c*. 50% higher than that of the permafrost soils (Extended Data Figure 1). However, experimental addition of nutrients (Supplementary Methods) to the permafrost soil did not affect cumulative CO_2 production (nutrients main effect ANOVA $F_{1,16}$=2.09 P=0.168, Extended Data Figure

6). It therefore is unlikely that relieving nutrient limitation by the (very small) addition of nutrients in inoculum soil has caused the observed increases in CO_2 production.

4. Is the increase in CO_2 production observed after soil transfer due to a priming effect of permafrost SOM decomposition induced by the addition of labile C and N compounds upon soil transfer?

No. First, amendment with an isotopically labelled labile carbon substrate (^{13}C-cellulose, 2g . kg soil DW^{-1} equivalent to *c*. 2.6 times more than total C introduced by soil transfer) caused only a small increase in cumulative SOM-derived CO_2 production of 8.9% (95% CI: 6.8 – 10.9%; ANOVA $F_{1,16}$=42.24, $P<10^{-4}$, n=3). Moreover, the magnitude of this priming effect was additive to the effect of the ST-treatment (cellulose:transfer interaction $F_{1,16}$=1.01, P=0.330, Extended Data Figure 6). Secondly, the labile C-induced priming effect was also independent of nutrient addition (cellulose:nutrient interaction $F_{1,16}$=0.02 P=0.890), and likewise there was no three-way interaction (cellulose:nutrient:transfer interaction $F_{1,16}$=0.02, P=0.887, Extended Data Figure 6). Lastly, the high TDC concentration in Yedoma sediment (350 mg TDC . kg soil DW^{-1}), i.e. *c.* nine times higher than in the donor soil suggests that the microbial community in the Yedoma sediment was not carbon-limited, and suggests against priming from the *c*. 0.3% of TDC introduced by soil transfer. The increase in CO_2 production with the ST-treatment effect therefore appears to be independent of priming effects and nutrient availability.

Supplementary Methods

1. ^{13}C-labelled cellulose and nutrient addition

To assess potential alternative explanations (priming effect, release of nutrient limitation) of the effect of soil transfer (ST) on CO_2 production from Yedoma permafrost, we amended Yedoma sediment with a full-factorial combination of isotopically labelled labile C (^{13}C-cellulose; to test for priming effects), nutrients (N, P, K; to test for nutrient limitation), and the exotic microbial community (ST), resulting in eight individual treatments (Extended Data Figure 6). CO_2 flux measurements were carried out as described in the Methods section, with additional measurements of CO_2 isotopic composition for the ^{13}C-cellulose treatments (Picarro g2131-*i* equipped with a small sampling module). The Vienna PDB standard was used for $\delta^{13}C$ calculations.

<u>^{13}C-labelled cellulose addition and isotopic partitioning</u>

^{13}C-cellulose was extracted from peas grown under a 100% ^{13}C-enriched atmosphere, and had a $\delta^{13}C$ value of 2210.885 (SE 0.716, n=2), while the Yedoma sediment $\delta^{13}C$ was -25.705 (SE 0.016, n=3). The use of ^{13}C-labeled cellulose allowed separation of total CO_2 production (R_t) into soil C (R_s) and cellulose (R_c) using the mass balance equations:

(1) $R_s + R_c = R_t$

(2) $^{13}A_s \times R_s + {}^{13}A_c \times R_c = {}^{13}A_t \times R_t$

Where $^{13}A_s$, $^{13}A_c$ and $^{13}A_t$ are the ^{13}C abundances in soil, cellulose and total CO_2 production, respectively. If we define $\alpha = R_c / R_t$, then:

(3) $\alpha = R_c / R_t = ({}^{13}A_t - {}^{13}A_s) / ({}^{13}A_c - {}^{13}A_s)$

And

(4) $R_s = (1 - \alpha) \times R_t$

Allowing us to calculate R_s as the soil organic matter-derived fraction of CO_2 production.

<u>Mineral nutrient addition</u>

To ensure an absence of nutrient limitations, soils were supplemented with a mixture of NH_4NO_3 – KH_2PO_4 (NPK) to reach a C:N ratio of 15:1, C:P ratio of 60:1 and C:K ratio of 150:1, as per Ref. 52. This nutrient addition accounted for the additional quantity of ^{13}C-labelled cellulose on the C pool size when both cellulose and nutrients were added. The pure donor soil was incubated only in presence of NPK addition (Extended Data Figure 6), where the dashed column represents the estimated value of CO_2 production upon incubation without NPK addition based on CO_2 production

rates for the donor soil with and without NPK addition from Ref. 52, assuming similar responses to NPK addition (17.15% decrease) at 20°C (in Ref. 52) and at 11°C (here).

2. Estimated CO_2 production of donor soil and ST treatment

To calculate how much more easily decomposable the donor soil should be to explain the CO_2 production increase induced by ST without functional limitations, we first calculated the average CO_2 production in control and ST soils (770.67 / 50 = 15.413 mg-C per jar and 1063.85 / 50 = 21.277 mg-C per jar, respectively, Figure 2a) and the difference between the two (5.864 mg-C per jar). The CO_2 production of the donor soil in absence of mineral nutrients addition (Extended Data Figure 6), was estimated by multiplying the cumulative CO_2 production of the measured 'donor soil + NPK' by 1.207 to account for the lower CO_2 production observed in presence of mineral nutrients, as per Fontaine *et al*., 2011 (Ref. 52). This estimated figure (dashed column in Extended Data Figure 6) is the one on which we base the calculations for Supplementary Discussion point 2 (e.g. 65% lower than the control soils). This allowed us to estimate the expected effect of the ST treatment assuming no biological interactions (green symbol in Extended Data Figure 6), by simply multiplying the baseline cumulative CO_2 production of control and donor soil on a w:w basis, i.e. 97.5% (control CO_2 production) + 2.5% (donor soil CO_2 production), *c*. 758.21 mg-C kg soil DW^{-1} (green dot in Extended Data Figure 6, about 1.8% lower than observed in the control soil).

We then used the elemental C content to calculate the average C content of the different fractions, as reported in Extended Data Figure 1. For the donor soil, average total C content was 626.00 mg-C, of which 0.78 mg-C were dissolved.

We then calculated the fraction of SOC that was mineralized after 161 days in control permafrost and in donor soil. For this we made the simplifying assumption that all dissolved C is labile and mineralized. Per jar:

- (15.413 – 7.01) / (610 – 7.01) = 1.39% of control SOC mineralized after 161 days;
- (272 / 50 – 0.78) / (626 – 0.78) = 0.74% of donor SOC mineralized after 161 days;

If we exclude biological interactions affecting Yedoma permafrost, the difference between the average measured 15.413 mg-C per jar (control soils) and the 21.277 mg-C per jar (ST soils) must come from the donor soil introduced during soil transfer. Still assuming that all dissolved C was mineralized, the difference in SOC mineralization between control and ST soils is as follows:

$(CO_2\text{-}_{ST} - TDC\text{-}_{ST}) - (CO_2\text{-}_{control} - TDC\text{-}_{control}) = (21.277 - 6.851) - (15.413 - 7.006) = 6.019$ mg-C

This amounts up to 38.5% of the SOC in the 0.5 g donor soil used for soil transfer. When incubated in isolation, 0.74% of the SOC in the donor soil is mineralized, this implies that to correspond to our observations, the donor soil microbes should mineralize the SOC of their own soil 52 times faster when incubated with Yedoma sediment than when incubated on their own soil. Alternatively, the Yedoma sediment microbes should mineralize the SOC of the donor soil 28 times faster than they mineralize the SOC in their own soil.

If we assume none of the dissolved C is mineralized, the figures change slightly: Yedoma and donor soil SOC mineralization become 2.53% and 0.87%, respectively, the difference in CO_2 production is 5.864 mg-C, or 37.5% of the 0.5 g donor soil SOC, meaning the donor soil and Yedoma microbes must mineralize the donor soil SOC respectively 43 and 15 times faster than they would mineralize their own soil, which are unrealistically large differences to the baseline CO_2 production measured when the soils are incubated in isolation.

3. Reproduced incubation

To further explore the potential of arctic active layer soils to alleviate functional limitations in Yedoma sediment, and the susceptibility of other permafrost soils to functional limitations, we performed two additional incubation experiments (Extended Data Figure 8). The active layer and permafrost soils were collected from the same locations in August 2012 (Franklin Bluffs), September 2015 (Storflaket) and August 2016 (Ice Cut), around the time of maximum thaw depth.

3a. Potential of different arctic active layer soils to alleviate functional limitations

The aim of this side-experiment was to compare the impact of different inocula, which might or might not alleviate functional limitations, on CO_2 production in Yedoma sediment. Excluding putative alleviation by microbes other than those found in the selected arctic topsoils was therefore more important here, than in our main experiment (evidencing the existence of functional limitations), and conditions closer to asepsis were applied for that reason. We further used liquid suspensions rather than soil transfer, to simulate downwards microbial migration through percolating water. The three active layer (AL) soils were a turbel (cryoturbated soil) and two histels (sedge peat and *Sphagnum* peat), as examples of soil and vegetation types found throughout the Yedoma domains of Alaska and Siberia[25].

The turbel soil was sampled from the center of a non-sorted circle in the coastal plain of the Alaskan North Slope (AL1, frost boil at Franklin Bluffs; gravimetric water content GWC 23.5% ± 1.2%; organic matter content OMC 6.82% ± 0.50%; mean ± SE, n = 3), the histel inocula from organic sedge peat at the boundary of the Yedoma domain of the Alaskan North Slope (AL2, moist non-acidic tundra at Ice Cut; GWC: 81.3% ± 2.0%; OMC: 86.81% ± 1.52%), and from a *Sphagnum* peat bog underlain by silty permafrost in sub-arctic Sweden (AL3, palsa mire at Storflaket; GWC: 79.1% ± 0.8%; OMC: 95.91% ± 0.09%). Lastly, we also used the donor soil used in our main experiment as a "positive control" known to be able to alleviate functional limitations (GWC: 25.8% ± 0.2%; OMC: 13.50% ± 0.16%). Active layer soils were collected with a breadknife and shovel or a peat-corer. The gravimetric water content (GWC) and organic matter content (OMC) of the soils were determined by drying *c*. 5g fresh soil at 105°C for at least 24h, and at 475°C for 4h, respectively.

Soil suspensions were prepared in autoclaved Erlenmeyer flasks with 50g (fresh weight) soil and 100mL (for the more mineral AL1 and ST soils) or 150 mL (organic AL2 and AL3 soils) autoclaved ddH_2O under a UV-cleaned and bleached laminar flow hood. Slurries soaked for 1 hour at 4°C were shaken for 90 min (150 rpm, orbital), stored overnight at 4°C, and then filtered through qualitative filter paper to remove large-sized particles (Ahlstrom-Munksjö, Eskilstuna, Sweden; 10 µm pore size, previously washed with autoclaved ddH_2O and air-dried to prevent cellulose leaching from the filter). TDC and TN were analyzed on filtered and acidified aliquots (0.45 µm, Filtropur S, Sarstedt AG & Co., Germany; 50 µL 20% HCl to 20 mL filtrate) by high temperature catalytic oxidation (HTCO) using a Shimadzu TOC-V CPH analyzer with a TN unit (Shimadzu Corporation, Japan). TDC and TN values per kg dry soil were 0.771 ± 0.018 mg C and 0.042 ± 0.001 mg N for AL1, 49.264 ± 5.118 mg C and 0.019 ± 0.002 mg N for AL2, 2.799 ± 0.198 mg C for AL3 (N below detection limit), and 0.681 ± 0.023 mg C and 0.477 ± 0.016 mg N for ST (one measurement per suspension, mean ± SE derived from differing soil weight across four jars).

A fourth core of Yedoma sediment, sampled simultaneously with the soil used in the main experiment (see Methods, 'Soil description and sampling'), was thawed overnight in a UV-treated and bleached positive pressure hood, then homogenized through a 2 mm sieve into a stainless steel basket, and excess water was decanted. Approximately 20 g (fresh weight) homogenized sediment was set in UV-treated jars, sealed with parafilm to allow for gas but not moisture or microorganism exchange, and pre-incubated at 10°C for 11 days before inoculation.

One mL of the respective soil suspensions was added to randomly-assigned jars for each of the four inoculum treatments (AL1, AL2, AL3 and ST inoculum) and one mL autoclaved ddH_2O was added to control jars. After 1 day, water-extractable pH was unaffected by the inoculation treatments (Kruskal-Wallis $\chi^2 = 4.807$, df = 4, $P = 0.308$; 2.5g soil FW in 40 mL, 250rpm orbital shaking for 2 hours, 10 µm qualitative filter as above).

3b. Functional limitations of different permafrost soils

We tested for the susceptibility of three additional permafrost soils to functional limitations, by inoculating them with the donor soil also used in our main experiment. We used permafrost soils from the sites described above for the active layer soil suspension inocula, since turbels and histels are important pools of permafrost SOC[1]. Because a large part of the circum-arctic was ice-covered until the Holocene, Yedoma deposits are the main type of permafrost preserved since the Upper Pleistocene. As such, microbial communities in Yedoma permafrost may be particularly affected by environmental filtering over long time-scales, while most extant permafrost, formed through the Holocene, would harbour microbial communities that have undergone shorter-term freezing constraints, and may not be as functionally-limited. At least two of the permafrost soils we tested in this additional incubations are more recent deposits than Yedoma: the turbel from Franklin Bluffs (Permafrost1; GWC: 19.5% ± 1.4%; OMC 1.18% ± 0.04%; mean ± SE, n = 4) lies further north than the boundary of the Alaskan Yedoma domain[25], while the soil from Storflaket (Permafrost3; GWC: 28.4% ± 0.4%; OMC 3.56% ± 0.05%) is a silty lacustrine deposit formed after the Scandinavian Ice Sheet retreat and its C was ^{14}C-dated to c. 9100 years BP[97,98]. The last soil (Ice Cut, Permafrost2; GWC: 40.2% ± 0.7%; OMC 12.80% ± 0.07%) lies at the northern boundary of the Alaskan Yedoma domain[25] and it is uncertain whether it belongs to a Yedoma unit or an overlying Holocene deposit.

The permafrost soils were collected with a SIPRE corer as described in Methods, except for Storflaket soil which was sampled with a fluid-less gas-powered concrete drill[98,99]. The soils were homogenized and pre-incubated as described above for the Yedoma sediment, after which we added one mL of the ST soil suspension described above to jars containing c. 20g fresh permafrost soil (n = 4), and one mL autoclaved ddH2O to control jars. At day 1, water-extractable pH was unaffected by inoculation (Welch's one-tailed t.tests $P > 0.05$, df = 6, pH measurement as described above).

3c. CO2 production measurements

The jars for both side experiments were incubated in the dark at 10°C for 389 days. CO_2 concentrations were measured (EGM-5, PP Systems, Amesbury, Massachusetts) at intervals ranging from 2 to 37 days, keeping $[CO_2]_{v:v}$ below 28,000 ppm to prevent a toxic CO_2 build-up. After each measurement, the jars were flushed with 0.45µm-filtered CO_2-free air moisturized at 10°C with a dew point generator (LI-COR Biosciences, Lincoln, Nebraska), for >90 s at 1L min^{-1}, i.e. with at least 10 times the volume of the jar.

References

1. Hugelius, G. *et al.* Estimated stocks of circumpolar permafrost carbon with quantified uncertainty ranges and identified data gaps. *Biogeosciences* **11**, 6573–6593 (2014).

25. Strauss, J. *et al.* Deep Yedoma permafrost: A synthesis of depositional characteristics and carbon vulnerability. *Earth-Sci. Rev.* **172**, 75–86 (2017).

52. Fontaine, S. *et al.* Fungi mediate long term sequestration of carbon and nitrogen in soil through their priming effect. *Soil Biol. Biochem.* **43**, 86–96 (2011).

96. Dalenberg, J. W. & Jager, G. Priming effect of some organic additions to 14C-labelled soil. *Soil Biol. Biochem.* **21**, 443–448 (1989).

97. Klaminder, J., Yoo, K., Rydberg, J. & Giesler, R. An explorative study of mercury export from a thawing palsa mire. *Journal of Geophysical Research: Biogeosciences* **113**, G04034 (2008).

98. Olid, C., Klaminder, J., Monteux, S., Johansson, M. & Dorrepaal, E. Decade of experimental permafrost thaw reduces turnover of young carbon and increases losses of old carbon, without affecting the net carbon balance. *Glob. Change Biol*. Online version of record (2020).

99. Väisänen, M. *et al.* Meshes in mesocosms control solute and biota exchange in soils: A step towards disentangling (a)biotic impacts on the fate of thawing permafrost. *Applied Soil Ecology* **151**, 103537 (2020).

Supplementary Table 1: Primers and conditions for the qPCR assays for the inhibition test, 16S rRNA and *amoA* functional genes and the PCR reactions for 16S and ITS libraries. The qPCR reactions were carried out in two technical replicates with an initial denaturation at 95 °C for 5 min, and cycles of denaturation at 95 °C for 15 s, annealing for 30 s and elongation at 72 °C. Standard curves were derived by serial dilutions of linearized plasmids containing cloned fragments of the specific genes in the range of 10^1-10^7 copies per reaction.

qPCR assay target	Target gene	Primer	Primer sequence 5' - 3'	Primer reference	Final primer conc.	Cycles	Annealing temp.	Elongation time	Standard curves R^2 / efficiency %
Inhibition	TOPO vector	M13F	GTAAAACGACGGCCAG		0.1 µM	35	55 °C	45 s	NA / NA
		M13R	CAGGAAACAGCTATGAC						
Prokaryotes	16S rRNA V3	341F	CCTACGGGAGGCAGCAG	Muyzer *et al.,* 1993	0.2 µM	35	55 °C	30 s	0.993 / 101.7
		534R	ATTACCGCGGCTGCTGGCA						0.997 / 102.5
Ammonia-oxidizing bacteria (AOB) *	*amoA*	amoA-1F	GGGGTTTCTACTGGTGGT	Rotthauwe *et al* ., 1997	0.5 µM	40	55 °C	40 s	0.998 / 87.8
		amoA-2R	CCCCTCKGSAAAGCCTTCTTC						0.997 / 86
Ammonia-oxidizing archaea (AOA) *	*amoA*	CrenamoA23f	ATGGTCTGGCTWAGACG	Tourna *et al* ., 2008	0.5 µM	40	55 °C	40 s	0.997 / 91.2
		CrenamoA616R	GCCATCCATCTGTATGTCCA						0.997 / 87.7
Complete ammonia oxidizers clade A ‡	*amoA*	comaA-244F	TAYAAYTGGGTSAAYTA	Pjevac *et al.,* 2017	2 µM	40	52 °C	30 s	0.997 / 88.2
		comaA-659R	ARATCATSGTGCTRTG						0.994 / 92.4
Complete ammonia oxidizers clade B †	*amoA*	comaB-244F	TAYTTCTGGACRTTYTA	Pjevac *et al.* , 2017	2 µM	40	52 °C	30 s	0.997 / 90.2
		comaB-659R	ARATCCARACDGTGTG						0.998 / 93.6
Total complete ammonia oxidizers §‡	*amoA*	Ntsp_amoA_162F	GGATTTCTGGNTSGATTGGA	Fowler *et al.* , 2018	0.5 µM	25	48 °C	45 s	0.993 / 92.3
		Ntsp_amoA_359R	WAGTTNGACCACCASTACCA						0.999 / 98.4

*Soil samples from the control were below detection limit (10 copies per reaction); †specific-size bands could not be obtained for soil samples from the control; ‡specific-size bands could not be obtained for any sample; §denaturation step in cycles was 45 s.

		16S rRNA gene V3 amplicons	ITS1 amplicons
Primers and sequences 5' - 3'		341F CCTACGGGAGGCAGCAG 518R* ATTACCGCGGCTGCTGG	ITS1f CTTGGTCATTTAGAGGAAGTAA ITS2* GCTGCGTTCTTCATCGATGC
Reference		Bartram *et al* ., 2011	Smith and Peay, 2014
Phusion High-Fidelity PCR Master Mi		12.5 µL	
Nuclease-free water		8 µL	
DNA template volume		2 µL	
DNA template dilution		5 ng . μL^{-1} or up to 1:50	
Primer concentration		10 µM	
Primer volume		1.25 µL	
Reaction volume		25 µM	
Initial denaturation		98 °C 1 min	98 °C 3 min
x35	Denaturation	98 °C 10 s	98 °C 30 s
	Annealing	58 °C 30 s	55 °C 30 s
	Elongation	72 °C 30 s	72 °C 45 s
Final elongation		72 °C 10 min	72 °C 5 min
PCR clean-up		AMPure XP Bead Clean-up (Beckman-Coulter, Brea, USA)	

* Reverse primers harboured indexes as per Bartram *et al*., 2011 and Smith and Peay, 2014